RIGOROUS A-POSTERIORI ERROR BOUNDS FOR POLYNOMIAL APPROXIMATIONS TO STABLE/UNSTABLE MANIFOLDS OF FIXED POINTS WITH APPLICATION TO ANALYTIC SHADOWING OF CONNECTING ORBITS FOR DISCRETE TIME DYNAMICAL SYSTEMS

J. D. MIRELES-JAMES* AND KONSTANTIN MISCHAIKOW†

Abstract. This work is concerned with high order polynomial approximation of stable and unstable manifolds for analytic discrete time dynamical systems. We develop 'a-posteriori' theorems for these polynomial approximations which allow us to obtain rigorous bounds on the truncation errors via a computer assisted argument. Moreover we repersent the truncation error as an analytic function, so that that the derivatives of the truncation error can be bound using classical estimates of complex analysis. As an application of these ideas we combine the approximate manifolds and rigorous bounds with a standard Newton-Kantorovich argument in order to obtain computer assisted proofs of the existence of connecting orbits between fixed points of discrete time dynamical systems. Examples of the manifold computation are given for invariant manifolds which have dimension between two and ten. Examples of the a-posteriori arguments and that analytic shadowing argument for connecting orbits are given for dynamical systems in dimension three and six.

1. Introduction. Suppose that $f : \mathbb{R}^n \to \mathbb{R}^n$ is real analytic in some neighborhood $N \subset \mathbb{R}^n$ of a hyperbolic fixed point $p \in N$. Then f is a local real analyticomorphism of N. Let $n_s, n_u \in \mathbb{N}$ denote respectively the dimension of the stable and unstable eigenspaces of $Df(p)$, and note that $n_s + n_u = n$. It follows from the stable manifold theorem [29] that there are $\nu_s, \nu_u, > 0$ and analytic chart maps

$$P : B_{\nu_u}(0) \subset \mathbb{R}^{n_u} \to \mathbb{R}^n \qquad \text{and} \qquad Q : B_{\nu_s}(0) \subset R^{n_s} \to \mathbb{R}^n$$

for the local unstable and stable manifolds at p, so that

$$P[B_{\nu_u}(0)] = W^u_{\text{loc}}(p) \qquad \text{and} \qquad Q[B_{\nu_s}(0)] = W^s_{\text{loc}}(p).$$

The *Parameterization Method*, developed by Cabré, de la Llave, and Fontich in [9, 10, 11] (and reviewed in Sections 2 and 3), provides an efficient method for computing N-th order power series approximations P_N and Q_N for the chart maps P and Q, as well as a general framework for establishing the convergence of such series.

In the present work we assume that the differential $Df(p)$ is diagonalizable and denote by Λ_s the $n_s \times n_s$ diagonal matrix of stable eigenvalues and by Λ_u the $n_u \times n_u$ diagonal matrix of unstable eigenvalues. The parameterization method is based on the fact that the chart maps P and Q satisfy the functional equations

$$f[P(\theta)] = P(\Lambda_u \; \theta) \qquad \text{and} \qquad f[Q(\phi)] = Q(\Lambda_s \; \phi) \tag{1.1}$$

for any $\theta \in B_{\nu_u}(0) \subset \mathbb{R}^{n_u}$ and $\phi \in B_{\nu_s}(0) \subset \mathbb{R}^{n_s}$. The fact that the chart maps satisfy functional equations is essential in the development of both the formal series approximations P_N and Q_N, and in the convergence analysis of the formal series.

*Rutgers University, Department of Mathematics, 110 Frelinghuysen Rd, Piscataway, NJ 08854, USA.

†Rutgers University, Department of Mathematics & BioMaPS, 110 Frelinghuysen Rd, Piscataway, NJ 08854, USA.

The main technical result of the present work is Theorem 4.1, which provides rigorous bounds on the truncation error $Q_N - Q$ (and similarly for the unstable manifolds). The estimates are 'a-posteriori' in the sense that the bounds we obtain are of the form

$$\sup_{\theta \in B_{\nu_s}} |Q(\theta) - Q_N(\theta)| \leq C(N) \sup_{\theta \in B_{\nu_s}} |f[Q_N(\theta)] - Q_N(\Lambda_s \theta)|, \tag{1.2}$$

where $C(N) \to 0$ as $N \to \infty$. The explicit form of $C(N)$ is given in Theorem 4.1. Since all terms on the righthand side of the Inequality (1.2) are explicitly know, and since the supremum on the righthand side of the inequality can be estimated using rigorous numerical methods, Theorem 4.1 can be used to obtain mathematically rigorous computer assisted bounds on the truncation errors associated with the polynomial approximations P_N and Q_N.

While the a-posteriori bounds obtained in Theorem 4.1 are interesting in their own right, we also show how they can be applied to the problem of computer assisted proof of the existence connecting orbits in discrete time dynamical systems. This leads to a scheme, presented in Section 5, which is best thought of as an a-posteriori validation method for the method of *projected boundary conditions*. The method of projected boundary conditions was developed for numerical approximation of heteroclinic and homoclinic orbits by Beyn and Kleinkauf in [7, 8]. The idea is as follows.

Suppose for the moment that $f : \mathbb{R}^n \to \mathbb{R}^n$ is invertible (see however Remark 1.1 below). Define the *homoclinic operator equation* $F : \mathbb{R}^{nk} \to \mathbb{R}^{nk}$ by

$$F(\theta, x_1, x_2, \ldots, x_{k-2}, x_{k-1}, \phi) = \begin{bmatrix} f^{-1}(x_1) - P(\theta) \\ f^{-1}(x_2) - x_1 \\ f^{-1}(x_3) - x_2 \\ \vdots \\ f^{-1}(x_j) - x_{j-1} \\ f(x_j) - x_{j+1} \\ \vdots \\ f(x_{k-2}) - x_{k-1} \\ f(x_{k-1}) - Q(\phi) \end{bmatrix} \tag{1.3}$$

where $\theta \in \mathbb{R}^{n_u}$, $\phi \in \mathbb{R}^{n_s}$, and $x_i \in \mathbb{R}^n$ for each $1 \leq i \leq k-1$. Here j is some fixed integer with $1 \leq j \leq k-1$. Then x_j is a point whose inverse iterates lie on the local unstable manifold, and whose forward iterates lie on the local stable manifold. Let $\tilde{x} = (\tilde{\theta}, \tilde{x}_1, \ldots, \tilde{x}_{k-1}, \tilde{\phi})$ denote a zero of F, then $O = \{P(\tilde{\theta}), \tilde{x}_1, \ldots, \tilde{x}_{k-1}, Q(\tilde{\phi})\}$ is an orbit segment which begins on the local unstable manifold of p and ends, after k iterates, on the local stable manifold of p. It follows that orbit(q) is homoclinic to p for any $q \in O$.

Now, if P_N and Q_N are polynomial approximations of the chart maps P and Q, then one defines F_N in analogy with Equation 1.3 by replacing the the exact chart maps with their polynomial approximations. The method of projected boundary conditions consists of numerically solving $F_N(x) = 0$ using a Newton Scheme, and enables fast and accurate numerical computation of connecting orbits.

Now suppose that $\hat{x}$ is an approximate zero of F_N, computed numerically as just described. Then it is natural to try to invoke the Newton-Kantorivich Theorem (Thm

4.3) in order to prove the existence of an exact zero $\tilde{x}$ near $\hat{x}$ of the full map F. The possibility of this kind of computer assisted proof of the existence of a connecting orbit is in fact mentioned in [7, 8]. Note that the map F is on $\mathbb{R}^{nk}$ so that the Newton-Kantorovich argument finite dimensional.

The difficulty in implementing this argument is the fact that we only know explicitly the map F_N, yet we want to prove the existence of a zero of the map F. In order to overcome this difficulty we require;

(i) rigorous bounds on the truncation errors in the approximations $P \approx P_N$ and $Q \approx Q_N$, so that we can bound the true residual $\|F(\hat{x})\|$.

(ii) rigorous bounds on the derivative of the truncation errors at the approximate solution $\hat{x}$, so that we can bound the derivative of F at $\hat{x}$.

(iii) rigorous uniform bounds on the second derivative of the truncation errors in a neighborhood of the approximate solution $\hat{x}$, so that we can bound DF in a neighborhood of $\hat{x}$.

We note that these are precisely the difficulties overcome by our a-posteriori results on the parameterization truncation errors. Once we use Theorem 4.1 in order to bound the truncation error (as an analytic function) we obtain the necessary bounds on the first and second derivatives of the truncation using a c Cauchy Type Bound from KAM theory.

Remarks 1.1 (EXTENSIONS).

1. The homoclinic operator equation given by Equation 1.3 can easily be modified to define an equation whose solution is a heteroclinic orbit between two distinct hyperbolic fixed points p_1 and p_2. This is done by taking P and Q to be respectively the parameterizations of the n_u dimensional unstable manifold at p_1 and the n_s dimensional stable manifold at p_2. As long as the manifolds satisfy the usual non-degeneracy conditions, namely $n_s + n_u = n$, then map F is non-degenerate and the method of projected boundary conditions is valid.

2. If f is not invertible, but p is a hyperbolic fixed point, then the local stable and unstable sets can still be defined and the stable manifold theorem generalizes as in [48]. Since p is hyperbolic, f is a local analyticomorphism and the parameterization method can still be used to compute the local manifolds. Of course the usual care must be take in globalizing the local stable manifold due to the non-existence of a unique inverse map. See [37, 38] for more complete discussion. At any rate, our a-posteriori scheme for computer assisted proof of the existence of connecting orbits can be applied to non-invertible maps as well. In the case that f is non-invertible, the parameterizations must be restricted to suitable neighborhoods of their fixed points, so that the image of the approximations P_N and Q_N do not intersect the singularity set of Df.

3. In the non-invertible case it is also natural to take $i = 1$ in the operator Equation 1.3 (or it's heteroclinic equivalent). That way only one application of an inverse map is needed. Of course the choice of inverse maps is dictated by the specific problem at hand (i.e. the approximate orbit whose existence is to be validated). For a more complete discussion of connecting orbits for non-invertible maps we refer to [49].

4. Finally note that the requirement that the map is real analytic can be lessened to piecewise real analytic (liner, polynomial, etc) and the methods presented here apply so long as all of the points $\hat{x}_i$, $\tilde{x}_i$, $1 \leq i \leq k-1$ are bounded away from the singularity set of Df.

The remainder of the paper is organized as follows. In Section 2 we discuss the background material used throughout the present work. We begin with a brief review of the parameterization method literature and a short discussion of the literature on computer assisted proof for the existence of connecting orbits in discrete time dynamical systems. In Section 2.1 we introduce the example dynamical systems used for the applications later in the paper.

In Section 3 we review the basic notions of the Parameterization Method for Stable and Unstable manifolds of fixed points of a local diffeomorphism f. We also give performance results for the numerical computation of the rigorous interval enclosure of the parameterization coefficients for a dimension dependent family of example maps which always have a one dimensional unstable manifold and a co-dimension one stable manifold. This allows us to examine the computational costs of computing the chart maps for invariant manifolds of dimension between two and ten.

Section 4 is devoted to the proof of Theorem 4.1, the main technical result of the present work. The section is organized as follows. In Section 4.1 we review the functional analytic and complex variables theory which is needed for the proof of Theorem 4.1, and in Section 4.2 we sketch the proof while introducing a series of Lemmas. In Seciton 4.3 we prove the lemmas in order to complete the proof of Theorem 4.1. Section 4.4 shows how to obtain one of the bounds in the hypothesis of Theorem 4.1 if the case that f is polynomial.

In Section 5 we apply the a-posteriori estimates of Theorem 4.1 to the Newton-Kantorovich problem associated with zeros of Equation 1.3. The main result is Theorem 5.1; our analytic shadowing theorem. The proof of Theorem 5.1 is a straight forward application of the Newton-Kantorivich theorem and is given in Section 5.2

In Section 6 we present the results of several computer assisted proofs of the existence of transverse homoclinic orbits in the three dimensional Lomelí Map. Here the stable and unstable manifolds are one and two dimensional respectively. We provide examples of the use of high order approximations to the manifold (useful when proving the existence of many distinct homoclinic orbits at a single parameter set) and low order approximation of the manifold (useful when continuing a single orbit over a range of parameters). In order to demonstrate that the algorithms can be applied in dimensions higher than three, we also provide a six dimensional example computation for a pair of coupled Lomelí Maps. Here the proof involves establishing the existence of a transverse homoclinic orbit in the intersection of a four dimensional unstable manifold and a two dimensional stable manifold.

2. Previous Work. The so called *Parameterization Method* of [9, 10, 11] provides a theoretical framework for studying the convergence of formal power series expansions of stable and unstable manifolds associated with fixed points of discrete and continuous time dynamical systems, under mild non-resonance conditions.

In [9] an existence theorem ([9] Theorem 1.1) is proved which gives, under quite general hypotheses, the existence of C^k chart maps for local stable and unstable manifolds of C^k local diffeomorphisms on Banach spaces. The proof is constructive and, as noted by the authors in the beginning of [9] Section 3, lends itself to a-posteriori analysis and computer assisted proof.

[11] gives a number of applications of the parameterization method, including some elementary proofs of theorems about invariant manifolds in the analytic category, C^0 invariant manifold theorems, and a rigorous treatment of "slow invariant manifolds". The proofs in [11] rely on the use of the implicit function theorem. As a consequence they are not constructive (with the exception of [11] Theorem 5.4 on the existence of stable and unstable manifolds of hyperbolic periodic orbits of vector

fields. This theorem is proven using the contraction mapping theorem, and explicit a-posteriori bounds are given). [10] develops optimal regularity results for the parameterization method with respect to system parameters in the C^k category.

In addition the parameterization method has been extend into a general method for studying a wide variety of invariant manifolds in dynamical systems theory. For example in [27, 28] a method is developed for computing invariant tori and their stable and unstable manifolds in quasiperiodic discrete time dynamical systems. In [34] the parameterization method is used to study KAM tori in symplectic maps without the use of the so called *action/angle coordinates*. In [36] the parameterization method is used to prove the existence of certain 'mixed-stability' invariant manifolds associated with hyperbolic fixed points of symplectic and volume preserving diffeomorphisms. These manifolds have some stable and some unstable directions and are not defined in terms of assymptotic behavior of the orbits. (Rather they are made up of orbits which 'spend a long time' near the fixed point before moving away). Some extensions to invariant tori of infinite dynamical systems are given in [21]. That the parameterization method can be extended to the study of center manifolds (at least in the case of a single eigenvalue of one) is shown in [5], while for example [26, 40, 6, 12, 13] give numerical applications of the theory. All of the work mentioned in the present paragraph are based on constructive arguments and can in principle be adapted for use in computer assisted proof.

The matter of obtaining rigorous error bounds of the truncation errors associated with polynomial approximations of stable and unstable manifolds has been studied by several authors.

[57, Johnson and Tucker(2011), 6]

Computer Assisted Proof for Connecting Orbits in Maps: In 1965 Smale showed that non-degenerate connecting orbits give rise to complicated behavior in discrete time dynamical systems [51]. Since then substantial effort has been directed toward the the dual problems of using computers to (i) detect, and (ii) prove the existence of transverse connecting orbits and complicated/'chaotic' behavior in specific nonlinear dynamical systems. The present work focuses on (ii); using the computer to prove the existence of transverse homoclinic orbits, once a suitable numerical approximation has been found.

We mention only the work of [7, 8] on numerical computation of approximate homoclinic orbits (as this work is closely related to ours) and then take for granted the entire classical numerical literature. However we will attempt a brief survey of existing methods for computer assisted proof of connecting/horseshoe dynamics for discrete time dynamical systems. We focus on so called *a-posteriori* methods of proof. These are methods which allow one to conclude from the existence of a "good enough" numerical approximation of an orbit, that there exists a true orbit nearby. We also give a brief discussion of the parameterization method literature, as this is the main tool which we use in order to control the local stable and unstable manifolds in the remainder of the paper.

C^0 **A-Posteriori Techniques for Topological Horseshoes:** There exist several computer assisted proof schemes which make use of only topological information and pass directly from floating point or combinatorial approximations of connecting orbits to the existence of horseshoe dynamics. These methods bypass the question of whether or not connecting orbits between fixed/periodic points actually exist. The methods can be classified in terms of how the phase space near the approximate connecting orbit is represented. This choice of representation will in turn influence which topological tools are used to give the a-posteriori results.

For example, if the phase space is discretized by combinatorial complexes (simplicial or cubical) then it is natural to use theorems of combinatorial topology in the a-posteriori analysis. The Discrete Conley Index is a powerful tool in this setting, and was used for example in [41, 42] to prove the existence of horseshoe dynamics for a Poincare section of the Lorenz system. [54] shows how to obtain a-posteriori verification of the existence of a horseshoe from the existence of a combinatorial approximation to a connecting orbit in a quite general setting. The arguments make use of a Lefschitz fixed point theorem for topological index pairs. These methods were used recently in [19] to obtain entropy bounds in the Hénon map.

On the other hand it is sometimes desirable to discretize the phase space by parallelograms which are aligned with the expanding and contracting directions of the system. [23, 24] have developed an a-posteriori technique based on covering relations in order to prove the existence of horseshoe dynamics. The a-posteriori argument uses the notion of local Brower degree. This method is exploited for example in [2, 3] in order to establish chaotic dynamics in the Restricted Three Body Problem and the Hénon-Heiles Hamiltonian respectively. Similar windowing methods have been developed by [32, 33] and also by [50]. These methods have been used for example to validate numerical experiments for the standard map [25].

Lipschitz-C^2 A-Posteriori Techniques for Invariant Manifolds and Transverse Homoclinic Orbits: If one wants to prove statements about connecting orbits (orbits with prescribed asymptotic behavior at the fixed/periodic points) then it is necessary to exploit some regularity near the fixed/periodic point. On the other hand, even if one is only interested in establishing the existence of chaotic dynamics, some degree of regularity is needed in order to apply analytic rather than topological arguments. We note that while the methods described here make some assumptions on the differentiability of f, none of them require (or exploit) more than two derivatives.

There exist several Lipschitz/low regularity methods for a-posteriori analysis of the local stable and unstable manifolds of fixed points. For example [59] develops an a-posteriori stable/unstable manifold theorem based on covering relations and cone conditions. This can be combined with the C^0 windowing methods mentioned above in order to obtain an a-posteriori scheme for heteroclinic and homoclinic connecting orbits. Such a strategy is used for example in [4] to study heteroclinic and homoclinic orbits in Hénon-Heiles, in [58] to study heteroclinic and homoclinic orbits and obtain entropy bounds for the Hénon map, and in [56] to study connecting dynamics on the Rossler attractor.

Covering-relation-plus-cone-condition methods have been extended in order to prove the existence of more general hyperbolic invariant sets in [14]. This generalization has been used recently by [15] to prove the existence of a center manifold in a celestial mechanics problem.

We also mention here the work of [43], where a rigorous box covering method for planar maps with real distinct eigenvalues is developed. The method is used to study homoclinic chaos in the standard map, by proving directly that the globalized stable and unstable manifolds intersect transversally.

Another method, which is similar to the methods developed in the present work in that it exploits high-order polynomial approximations of the stable and unstable manifold, is developed in [57]. Here the invariant manifolds are approximated by 'Taylor Models'. Existence of the manifolds and a-posteriori bounds on the Taylor Model errors are proved via a nonlinear-box covering argument, which is topological rather than analytical. The method has been used in [44] to study connecting orbits and obtain entropy bounds for the Hénon map.

Finally we mention another thread in the literature which is based on analytical a-posteriori (or shadowing) arguments rather than topological methods. The main tool in this branch of the literature is the method of *exponential dichotomies*. In [53], an a-posteriori method is developed for proving the existence of a horseshoe given the existence of two numerically computed periodic orbits which pass near one another at a point. The a-posteriori argument is used to prove the existence of a horseshoe in the Hénon map. An extension of the method is given in [46] which allows exponential dichotomy arguments to be applied to homoclinic and heteroclinic orbits. The method is implemented in [17] and used to prove the existence of transverse hetero and homoclinic orbits in both the dissipative and area preserving Hénon map, as well as in the Cremona map.

Remarks 2.1.

a. While our method is closely related to the work of [46] we mention some differences. The methods of [46] require only C^2 assumptions, and as such they apply to a larger family of maps than the C^ω tools developed here.
On the other hand, exponential dichotomy arguments require a delicate local analysis near the fixed point (tail of the homoclinic orbit) in order to be able to apply a Newton-Kantorovich argument on an infinite dimensional sequence space. It is reasonable to think that if the dynamical systems of interest is C^ω, then the use of C^ω tools could provide some simplification of the arguments. We will show that this is the case; that when the dynamical system is C^ω we can replace the asymptotic segments of the orbit with a suitable approximation of the local stable and unstable manifolds, and formulate the entire problem in terms of a finite orbit segments which transition between the local manifolds. The resulting operator equation is finite dimensional, so that in the we obtain shadowing using only the finite dimensional Newton-Kantorovich Theorem.
In addition, using high order approximations of the local stable and unstable manifolds lets us work with orbit segments which begin and end farther from the fixed point. This allows us to avoid considering iterates of the map near the fixed point, where the dynamics are slow (and well understood). In principe this should allow for the study of orbits which spend a long time in transition from the local stable to the local unstable manifolds.

b. One could criticize the shadowing method presented here on the grounds that it cannot be applied to differential equations, as Poincare and time-τ maps of analytic vector fields need not be analytic, and in any case the explicit form of the mapping f is not explicitly known when f is a time-τ map. We answer this criticism by pointing to the recent work of [6], which shows how the techniques developed here can also be applied to differential equations.
The main idea in [6] is to work with an operator equation defined in the full phase space, rather than with a first return or time-τ map. The validated approximation to the connecting orbits obtained using this method are piecewise analytic arcs in phase space with rigorous error bounds along the entire arc (rather than only at the mesh or return points). We note also that the methods of [6] do not require rigorous integration of the system. Rather, as in the present work, a projected boundary value problem is solved using fixed point methods.

C^ω **A-Posteriori Techniques in KAM Theory and Celestial Mechanics:** Since the techniques developed in the present work are tailored for real analytic dynamical systems, our methods have much in common with the tools used by the numerical KAM and rigorous normal form communities, where working in the analytic category is common. For example a key component in the work of [55] is the use of a rigorous, high-order normal form about the equilibria at the origin of the Lorenz system. Since the normal form is used not simply as a computational tool, but rather as a critical ingredient in a computer assisted proof, it is necessary for the author to rigorously bound the truncation error associated with the coordinate change as well as its derivative and inverse (see [55] Proposition 3.1 as well as Lemmas 3.2 and 3.3).

Similar techniques are used in numerical KAM theory. See for example [16, 22] where stability of solar system astroids is studied by computing high-order normal forms about invariant tori in n-body problems. Again, since the authors are interested in computer assisted proofs they are required to rigorously bound the truncation errors in their expansions. In numerical KAM problems these bounds are usually obtained using analytical rather than topological methods. For a more thorough discussion of the numerical KAM literature see [35] and also [16].

Remark 2.1. Rigorous normal form and KAM computations typically involve the so called *small divisors* which arise due to resonant terms in the formal expansions. Overcoming the small divisors and proving the convergence of the formal series of KAM theory requires the use of powerful functional analytic tools (Nash-Moser quadratic convergence schemes, delicate majorant arguments, etc.) When studying formal expansions of stable and unstable manifolds, certain generic non-resonance conditions can be used to rule out small divisors above a certain finite order (see [9, 10, 11] and Section 3 below). Then the non-resonance conditions must only be checked numerically to finite order in order to obtain convergence of the formal series. This greatly simplifies the a-posteriori analysis.

2.1. Example Systems. For the numerical work in this paper we consider several maps which are derived from the classical Hénon map. The *delayed Hénon Map* is introduced in [52], and defined by

$$f(x_1, \ldots, x_n) = \begin{pmatrix} 1 - a\, x_1^2 + b\, x_n \\ x_1 \\ \vdots \\ x_{n-1} \end{pmatrix}. \tag{2.1}$$

The map is useful for producing examples of invariant manifolds of arbitrarily high dimension. The map has two fixed points $p_1, p_2 \in \mathbb{R}^n$ where

$$p_{1,2} = (x_\pm, \ldots, x_\pm) \qquad \text{with} \qquad x_\pm = b - 1 \pm \frac{\sqrt{(1-b)^2 + 4a}}{2a}.$$

We take $a = 1.6$ and $b = 0.1$ as in [52], so that p_1 has a one dimensional unstable manifold and an $n-1$-dimensional stable manifold for any phase space dimension n. In section (SOMETHING) we compute the coefficients for the $n-1$ dimensional stable manifold of p_1 using interval arithmetic for various phase space dimensions n and various parameterization orders N.

We also consider the five parameter family of (quadratic) volume preserving diffeomorphisms $f : \mathbb{R}^3 \to \mathbb{R}^3$ given by

$$f(x, y, z) = f_{\alpha,\tau,a,b,c}(x, y, z) = \left(\begin{array}{c} z + Q_{\alpha,\tau,a,b,c}(x, y) \\ x \\ y \end{array} \right), \tag{2.2}$$

where Q is the quadratic function

$$Q_{\alpha,\tau,a,b,c}(x, y) = \alpha + \tau x + ax^2 + bxy + cy^2, \qquad \text{with} \qquad a + b + c = 1. \tag{2.3}$$

This family of maps is useful for generating arbitrarily long homoclinic orbits, i.e. homoclinic orbits which require higher and higher numbers of iterates to make the excursion out of and then back to some fixed neighborhood of a fixed point (such an excursion is finite, as the fixed neighborhood isolates the asymptotic behavior at the fixed point). The family of maps was introduced in [39], as a volume preserving analog of the two dimensional area preserving Hénon map. We will refer to this as the *Lomelí Map*.

Note that when $\tau^2 - 4\alpha > 0$ the map has a pair of (real) distinct fixed points $p_\pm \in \mathbb{R}^3$

$$p_\pm = \left(\begin{array}{c} x_\pm \\ x_\pm \\ x_\pm \end{array} \right), \qquad \text{where} \qquad x_\pm = \frac{-\tau \pm \sqrt{\tau^2 - 4\alpha}}{2}.$$

These are the only possible fixed points of the family. We also note that it is possible to work out explicit formulas for f^{-1}, Df and Df^{-1} as functions of x, y, z.

An affine change of variables puts the Lomelí map in the form

$$g(x, y, z) = \left(\begin{array}{c} x + y \\ y + z - \epsilon + \mu y + P(x, y) \\ z - \epsilon + \mu y + P(x, y) \end{array} \right), \tag{2.4}$$

where $P(x, y) = \bar{a}x^2 + \bar{b}xy + \bar{c}z^2$. This form if the map is used in [20] and has the advantage that the two fixed points are located on the z-axis at $\pm\sqrt{\epsilon/\bar{a}}$, and that the map is more easily seen to converge to a (singular) integrable limit as ϵ approaches zero. We refer to this the "Dullin-Meiss" form of the map. In what fallows we will use the standard form of the Lomelí map in our numerical applications, largely so that we can exploit the computational tools and formula developed in [40]. Nevertheless the intuition provided by the Dullin-Meiss form is useful for understanding the dynamics of the family, and in particular for finding parameters with long homoclinic orbits.

Given a set of parameters in Dullin-Meiss form, it is possible to transform to a Lomelí Map with the parameters

$$\begin{aligned}
a &= \bar{c} \\
c &= \bar{c} + \bar{a} - \bar{b} \\
b &= \bar{b} - 2\bar{c} \\
\tau &= \frac{2\bar{a}(3+\mu)}{2\bar{a} - \bar{b}} \\
\alpha &= \frac{(9+6\mu+\mu^2)\bar{a} - 4\epsilon\bar{a}^2 + 4\epsilon\bar{a}\bar{b} - \epsilon\bar{b}^2}{(2\bar{a}-\bar{b})^2}.
\end{aligned}$$

These transformations allow us to relate the numerical studies carried out in this work, where we work with the Lomelií form of the map, with the numerical studies in [20]. In particular, we have that as ϵ approaches zero, the one dimensional stable manifold of p_+ and unstable manifold of p_- pass nearer and nearer to one another (the coincide in the integrable limit), causing homoclinic orbits of p_+ to "stagnate" for increasingly long periods of time near p_-. The stagnation period can be made arbitrarily long, so that proving the existence of the associated homoclinic orbits becomes an increasing computational challenge (see Section 6). This behavior is due to the fact, discussed at length in [20], that as ϵ approaches zero the Lomelí Map approaches an integral limit and in the integrable limit the one dimensional manifolds of the fixed points coincide.

Remarks 2.2 (Chaos and the Lomelí Map). There exists extensive numerical evidence that the Lomelí map admits chaotic motions for many parameter values. See for example Figures 7, 8, 22, and 28 in [20]. Our Figures 2.1 and 2.2 illustrate the stable and unstable manifolds of of the of p_1 for the Lomelí map, at a large and a small value of Dullin-Meiss ϵ. In both figures we can clearly see what appear to be several transverse intersections of the stable and unstable manifolds, indicating both the existence of homoclinic orbits and topological horseshoes for the Lomelí Map. In Section 5 we prove the existence of transverse homoclinic orbits, and thus chaos, for several specific parameter values.

Finally, in Section 6 we couple two Lomelí maps

$$\begin{aligned}
f_1(x_1, y_1, z_1) &\equiv f_{\alpha_1,\tau_1,a_1,b_1,c_1}(x_1, y_1, z_1) \\
&\text{and} \\
f_2(x_2, y_2, z_2) &\equiv f_{\alpha_2,\tau_2,a_2,b_2,c_2}(x_2, y_2, z_2)
\end{aligned}$$

in order to obtain the six-dimensional dynamical system $G : \mathbb{R}^6 \to \mathbb{R}^6$ given by

$$G(x_1, y_1, z_1, x_2, y_2, z_2) \equiv \left[\begin{array}{c} f_1(x_1, y_1, z_1) + \varepsilon g_2(y_2,) \\ f_2(x_2, y_2, z_2) + \varepsilon g_1(y_1) \end{array} \right], \tag{2.5}$$

where

$$g_1(y_1) \equiv (y_1 - x_1^+)(y_1 - x_1^-) \quad \text{and} \quad g_2(y_2) \equiv (y_2 - x_2^+)(y_2 - x_2^-).$$

Here $x_{1,2}^\pm$ denotes a coordinate of the fixed points in the $f_{1,2}$ systems (recall that the fixed points are on the $x = y = z$ line so that it is enough to specify only the x coordinate of the fixed point). Note that this coupling does not move the fixed points in the $f_{1,2}$ systems, but does change the eigenvalues and eigenvectors. When ε is small we can approximate a connecting orbit for G by taking the product of connecting orbits for $f_{1,2}$. This coupled map is useful for demonstrating that our scheme can be used to compute connecting orbits for higher-dimensional systems.

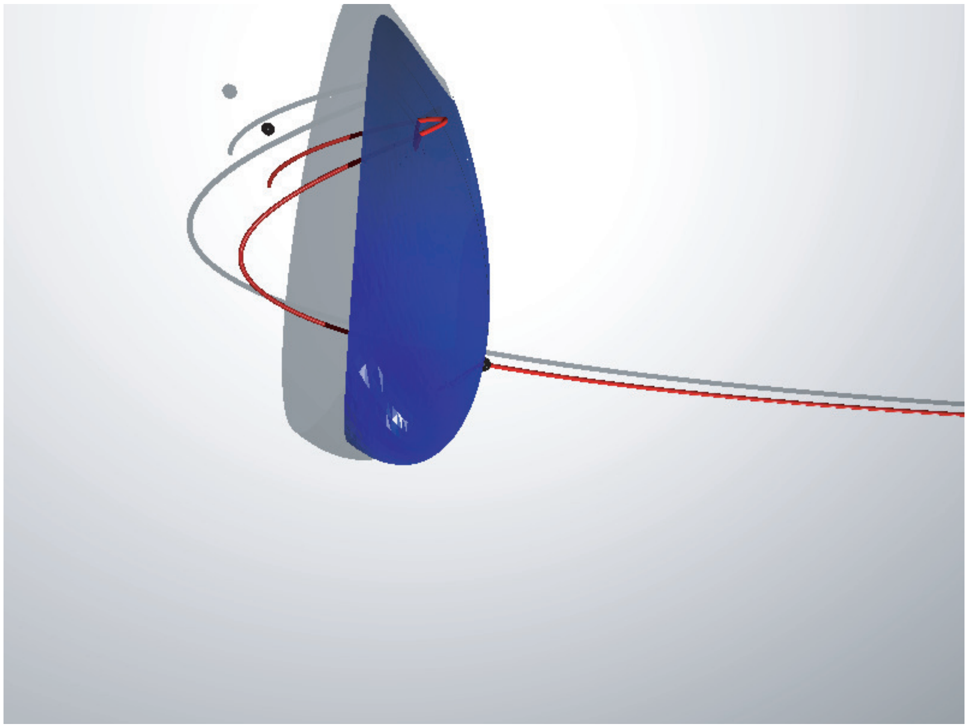

FIG. 2.1. *Apparent intersection of the stable and unstable manifolds for Dullin-Meiss parameter $\epsilon = 4$. The black spheres denote the fixed points p_1 and p_2. The blue is the two dimensional unstable manifold, and the red is the one dimensional stable manifold, both of p_1.*

3. Parameterization Method. In this section we review the Parameterization Method of [9, 10, 11]. We focus on the case where the map f is real analytic on a ball, the differential is diagonalizable, and there are no resonances between eigenvalues of like stability (these assumptions will be formalized below). For a more complete and general reference to the Parameterization method, the reader should consult [9, 10, 11].

More formally we take $p \in \mathbb{R}^n$ to be a hyperbolic saddle for the real analytic map $f : \mathbb{R}^n \to \mathbb{R}^n$. We assume that f is a local real analyticomorphism and uniformly bound on $B(p, \rho) \subset \mathbb{R}^n$. We also assume that that $Df(p)$ is diagnolizable over $\mathbb{C}$. Then $Df(p)$ has n_s distinct stable eigenvalues $\{\lambda_1^s, \ldots, \lambda_{n_s}^s\}$ with $|\lambda_i^s| < 1$, and n_u distinct unstable eigenvalues $\{\lambda_1^u, \ldots, \lambda_{n_u}^u\}$ with $|\lambda_i^u| > 1$, and $n_s + n_u = n$ as p is a saddle. We choose eigenvectors $\{\xi_1^s, \ldots, \xi_{n_s}^s\}$ and $\{\xi_1^u, \ldots, \xi_{n_u}^u\}$ associated with the stable and unstable eigenvalues respectively. For the moment we leave the lengths of the eigenvectors unspecified.

As mentioned in the introduction, the stable manifold theorem gives that $W^s(p)$ and $W^u(p)$ are n_s and n_u dimensional manifolds, respectively tangent to $\text{span}\{\xi_i^{n_s}\}$ and $\text{span}\{\xi_i^{n_u}\}$ at p. The goal of the parameterization method is to determine analytic mappings $Q : B(0, \nu_s) \subset \mathbb{R}^{n_s} \to \mathbb{R}^n$ and $P : B(0, \nu_u) \subset \mathbb{R}^{n_u} \to \mathbb{R}^n$ which parameterize the local stable and unstable manifolds $W^s_{\text{loc}}(p)$ and $W^u_{\text{loc}}(p)$ respectively at p. For the moment we focus our attention on the development of Q, and consider P at the end of the section.

We simplify our notation a little by letting $B_s \equiv B(0, \nu_s) \subset \mathbb{R}^{n_s}$, and Λ denote the $n_s \times n_s$ matrix with λ_i^s in the i-th diagonal entry and zeros elsewhere (this was

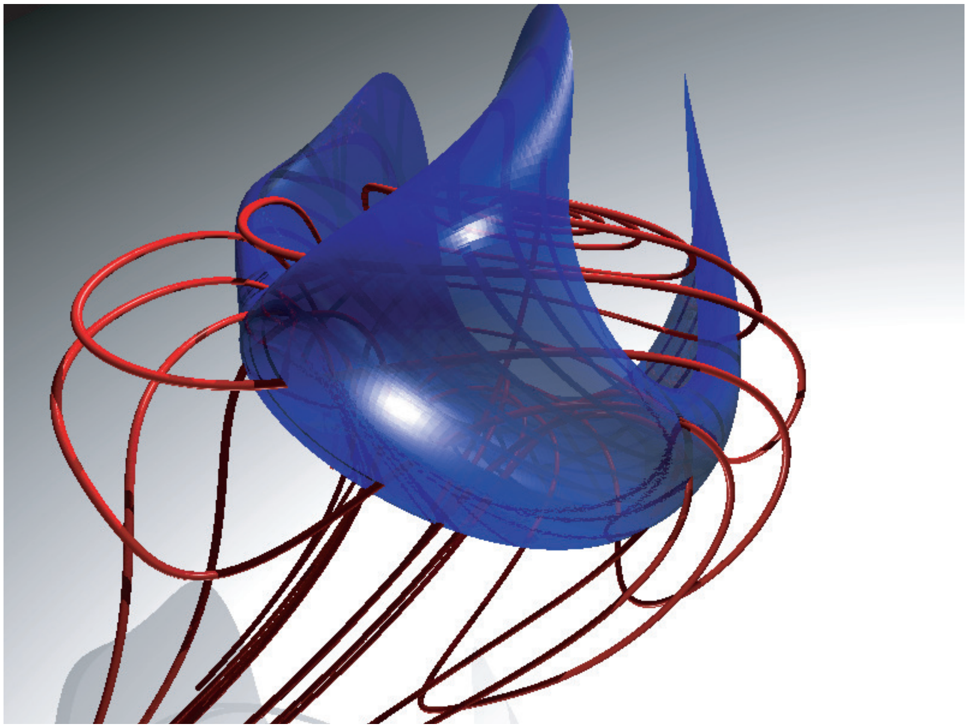

FIG. 2.2. *Apparent homoclinic tangle for Dullin-Meiss parameter ϵ near 1. The blue is the two dimensional unstable manifold, and the red is the one dimensional stable manifold, both of p_1.*

called Λ_s above). Then $Q[B_s]$ is a local stable manifold for p if and only of Q satisfies the following functional equation with initial data

1. $Q(0) = p$,
2. $DQ(0) = [\xi_1^s | \dots | \xi_{n_s}^s]$,
3. and

$$f[Q(\theta)] = Q(\Lambda\theta), \tag{3.1}$$

for all $\theta \in B_s$.

To see this note that for any Q satisfying these conditions, image(Q) is an immersed n_s-disk containing p and is tangent to span$\{\xi_i^{n_s}\}$ at p. Moreover Equation (3.1) implies that $(f \circ Q)(B_s) = Q[\Lambda B_s] \subset Q(B_s)$, so that the ω-limit set of image(Q) under f is p. Then

$$Q(B_s) = W^s_{\text{loc}}(p),$$

by definition.

In general it is impossible to compute Q in closed form. Instead, we note that Q satisfies a (functional) initial value problem with analytic data. Then it is natural to seek a power series expansion for Q of the form

$$Q(\theta) = \sum_{|\alpha| \geq 0} a_\alpha \theta^\alpha \qquad a_n \in \mathbb{R}^n, \quad \theta \in \mathbb{R}^{n_s}, \quad \alpha \in \mathbb{N}^{n_s} \tag{3.2}$$

convergent on B_s. Note that the first order constraints on Q demand that $a_{(0,\ldots,0)} = p$ and $a_{e_i} = \xi_i^s$ (here e_i is the multi-index with one in the i-th component and zeros elsewhere). Then the problem is to try to determine the unknown coefficients a_α for $|\alpha| \geq 2$.

REMARK 3.1. [Uniqueness] Note that the choice of the lengths of the eigenvectors ξ_i is free in the above formulation. This corresponds to the freedom in the choice of scaling of the parameterization of any manifold. Nevertheless, it is shown in [9] (and we will see again in Section 4) that the solution of Equation 3.1 is unique once the scale of the eigenvectors is fixed.

A formal solution of Equation (3.1) can be obtained by inserting the power series given by Equation (3.2) into Equation (3.1), expanding f as a power series, and computing recurrence relations for the coefficients of Q by matching like powers of θ. This approach is works especially when f is a polynomial map of low to moderate degree. Iterative approaches for solving Equation 3.1 are discussed in [9]. Numerical implementations of iterative algorithms for solving Equation 3.1 can be found in [40, 57, 44].

Finally, we note that the parameterization P of the local unstable manifold for f at p parameterizes the local stable manifold for f^{-1} at p, so that P must satisfy the functional equation

$$f^{-1} \circ P = P \circ \Omega^{-1}, \tag{3.3}$$

where Ω is the matrix of unstable eigenvaules of $Df(p)$. But if we right compose Equation (3.3) with Ω and left compose with f then we obtain

$$P \circ \Omega = f \circ P,$$

which is identical to Equatoin 3.1. Then P and Q solve the same functional equation, modulo the appropriate choose of linear map Λ or Ω.

3.1. Formal Computations for 1D Manifolds of the Lomelí Map. In order to illustrate the flavor of the formal computation of the power series coefficients for the stable/unstable manifold parameterizations we now consider the one-dimensional case for the Lomelí map

$$f(x, y, z) = \left(\begin{array}{c} \alpha + \tau x + z + a x^2 + bxy + cy^2 \\ x \\ y \end{array} \right).$$

Let p_0 denote either one of the fixed points of the map and recall that generically p_0 will have either a one dimensional stable eigenspace, or a one dimensional unstable eigenspace. Let

$$P(\theta) = \left(\begin{array}{c} P_1(\theta) \\ P_2(\theta) \\ P_3(\theta) \end{array} \right) = \left(\begin{array}{c} \sum_{n=0}^\infty v_n^1 \theta^n \\ \sum_{n=0}^\infty v_n^2 \theta^n \\ \sum_{n=0}^\infty v_n^3 \theta^n \end{array} \right), \tag{3.4}$$

be the unknown parameterization function for the one dimensional stable or unstable manifold, and let λ and ξ be the associated stable or unstable eigenvalue and eigenvector. Then $(v_0^1, v_0^2, v_0^3)^T = p_0$, and $(v_1^1, v_1^2, v_1^3)^T = \xi$ are the zero-th and first order power series coefficients.

Substituting the power series into Equation 3.1 gives

$$f \circ P = \begin{pmatrix} \alpha + \tau P_1 + P_3 + a[P_1]^2 + bP_1P_2 + c[P_2]^2 \\ P_1 \\ P_2 \end{pmatrix}$$

on the left, and

$$P(\lambda\theta) = \begin{pmatrix} \sum_{n=0}^{\infty} v_n^1 (\lambda\theta)^n \\ \sum_{n=0}^{\infty} v_n^2 (\lambda\theta)^n \\ \sum_{n=0}^{\infty} v_n^3 (\lambda\theta)^n \end{pmatrix} = \begin{pmatrix} \sum_{n=0}^{\infty} v_n^1 \lambda^n \theta^n \\ \sum_{n=0}^{\infty} v_n^2 \lambda^n \theta^n \\ \sum_{n=0}^{\infty} v_n^3 \lambda^n \theta^n \end{pmatrix}$$

on the right. Equating the second and third components of the left and right hand sides gives

$$\sum_{n=0}^{\infty} v_n^1 \theta^n = \sum_{n=0}^{\infty} v_n^2 \lambda^n \theta^n,$$

and

$$\sum_{n=0}^{\infty} v_n^2 \theta^n = \sum_{n=0}^{\infty} v_n^3 \lambda^n \theta^n.$$

Upon matching like powers this is

$$v_n^1 - v_n^2 \lambda^n = 0 \qquad\qquad v_n^2 - v_n^3 \lambda^n = 0. \tag{3.5}$$

The first component equation is more involved. Expanding the left hand side of the first component and utilizing the Cauchy product formula gives

$$\alpha + \tau \sum_{n=0}^{\infty} v_n^1 \theta^n + \sum_{n=0}^{\infty} v_n^3 \theta^n$$

$$+a \left[\sum_{n=0}^{\infty} v_n^1 \theta^n \right]^2 + b \left[\sum_{n=0}^{\infty} v_n^1 \theta^n \right] \left[\sum_{n=0}^{\infty} v_n^2 \theta^n \right] + c \left[\sum_{n=0}^{\infty} v_n^2 \theta^n \right]^2$$

$$= \alpha + \sum_{n=0}^{\infty} \tau v_n^1 \theta^n + \sum_{n=0}^{\infty} v_n^3 \theta^n$$

$$+ \sum_{n=0}^{\infty} \left(\sum_{k=0}^{n} a v_k^1 v_{n-k}^1 \right) \theta^n + \sum_{n=0}^{\infty} \left(\sum_{k=0}^{n} b v_k^1 v_{n-k}^2 \right) \theta^n + \sum_{n=0}^{\infty} \left(\sum_{k=0}^{n} c v_k^2 v_{n-k}^2 \right) \theta^n$$

$$= \sum_{n=0}^{\infty} v_n^1 \lambda^n \theta^n.$$

Equating like powers gives that for $n \geq 2$ we have that

$$\tau v_n^1 + v_n^3 + 2av_0^1 v_n^1 + bv_0^2 v_n^1 + bv_0^1 v_n^2 + 2cv_0^2 v_n^2$$

$$+ \sum_{k=1}^{n-1} \left[av_k^1 v_{n-k}^1 + bv_k^1 v_{n-k}^2 + cv_k^2 v_{n-k}^2 \right]$$

$$= \lambda^n v_n^1,$$

where we have removed from the sum any terms containing v_n^1, or v_n^2. We isolate the n-th order coefficients on the left hand side of the equality in order to obtain

$$(\tau + 2av_0^1 + bv_0^2 - \lambda^n) v_n^1 + (bv_0^1 + 2cv_0^2) v_n^2 + v_n^3$$

$$= -\sum_{k=1}^{n-1} \left[av_k^1 v_{n-k}^1 + bv_k^1 v_{n-k}^2 + cv_k^2 v_{n-k}^2 \right]$$

Combining the three component equations in matrix form gives

$$A_n \begin{bmatrix} v_n^1 \\ v_n^2 \\ v_n^3 \end{bmatrix} = \begin{bmatrix} s_n \\ 0 \\ 0 \end{bmatrix}$$

where

$$A_n = \begin{pmatrix} \tau + 2av_0^1 + bv_0^2 - \lambda^n & bv_0^1 + 2cv_0^2 & 1 \\ 1 & -\lambda^n & 0 \\ 0 & 1 & -\lambda^n \end{pmatrix} \tag{3.6}$$

and

$$s_n = -\sum_{k=1}^{n-1} \left[av_k^1 v_{n-k}^1 + bv_k^1 v_{n-k}^2 + cv_k^2 v_{n-k}^2 \right].$$

Note that if we let $y_n = (s_n, 0, 0)^T$, then the matrix equation has the form

$$\left[Df(p_\pm) - \lambda^n I \right] v_n = y_n. \tag{3.7}$$

This expression is seen to be correct by evaluating the formula for the Jacobian of the Lomelí Map at $p_0 = (v_0^1, v_0^2, v_0^3)$. Equation (3.7) is called the *homological equation* for the one dimensional stable manifold.

Then the coefficient v_n is well defined whenever A_n is invertible. But Equation 3.7 shows that A_n has the form of the characteristic matrix $Df(p_0) - \tau I$ of $Df(p_0)$, and the characteristic matrix is invertible precisely when τ is not an eigenvalue of $Df(p_0)$. Now, if λ is stable and the rest of the eigenvalues are unstable then $|\lambda| < 1 < |\lambda_i|$ so that $|\lambda^n| < |\lambda| < |\lambda_i|$ for all $n > 1$ (a similar arguments holds if $|\lambda| > 1$ and the remaining eigenvalues are stable). Then λ^n is never an eigenvalue of $Df(p_0)$ and the series solution $\sum v_n \theta^n = P(\theta)$ is formally well defined to all orders.

Remark 3.2.

- The computation above provides a numerical scheme for computing approximations to the stable manifold. Namely, we can compute a polynomial P_N which approximates P to any desired finite order by recursively solving the homological Equation (3.7) for $2 \le n \le N$.
- The magnitude of $\xi = v_1$ is free in the preceding discussion. This can be used to control the growth of the coefficients of P in numerical computations.
- We treat the convergence of the formal series defined by Equations 3.4 and 3.7 in Theorem 4.1.

3.2. Formal Computation of Two Dimensional Manifolds for the Lomelí Map. In order to parameterize a two dimensional (stable or unstable) manifold associated with a pair of real, distinct (stable or unstable) eigenvalues λ_1, λ_2, of $Df(p_0)$, having $|\lambda_1|, |\lambda_2| < 1$, we choose associated eigenvectors ξ_1 and ξ_2 and assume that the parameterization $P : \mathbb{R}^2 \to \mathbb{R}^3$ has power series expansion

$$P(\theta_1, \theta_2) = \sum_{n=0}^{\infty} \sum_{m=0}^{\infty} v_{mn} \theta_1^m \theta_2^n,$$

where $v_{mn} \in \mathbb{R}^3$ are coefficients having

$$v_{00} = p_{\pm}, \qquad v_{10} = \xi_1 \qquad \text{and} \qquad v_{01} = \xi_2.$$

The remaining v_{mn}, $m + n \ge 2$, are determined by requiring that P satisfy the functional equation $f \circ P = P \circ \Lambda$ which in this case is

$$f[P(\theta_1, \theta_2)] = P(\lambda_1 \theta_1, \lambda_2 \theta_2).$$

If we let $v_{mn} = (v_{mn}^1, v_{mn}^2, v_{mn}^3)^T$, then a formal computation similar to the one given in Section 3.1 shows that the coefficients for a two dimensional (stable or unstable) manifold solve the homological equation

$$\begin{pmatrix} \tau + 2a v_{00}^1 + b v_{00}^2 - \lambda_1^m \lambda_2^n & b v_{00}^1 + 2c v_{00}^2 & 1 \\ 1 & -\lambda_1^m \lambda_2^n & 0 \\ 0 & 1 & -\lambda_1^m \lambda_2^n \end{pmatrix} \begin{pmatrix} v_{mn}^1 \\ v_{mn}^2 \\ v_{mn}^3 \end{pmatrix} = \begin{pmatrix} -s_{mn} \\ 0 \\ 0 \end{pmatrix}, \quad (3.8)$$

where

$$s_{mn} = \sum_{j=0}^{n}\sum_{i=0}^{m} a\,\bar{v}^1_{(m-i)(n-j)}\bar{v}^1_{ij} + b\,\bar{v}^1_{(m-i)(n-j)}\bar{v}^2_{ij} + c\,\bar{v}^2_{(m-i)(n-j)}\bar{v}^2_{ij}$$

and

$$\bar{v}^s_{k\ell} = \begin{cases} 0 & \text{if } \; k = m \text{ and } \ell = n \\ v^s_{k\ell} & \text{otherwise} \end{cases}$$

for $s = 1, 2, 3$.

Remark 3.3.

- If a fixed point of the Lomelí map has a complex conjugate pair of eigenvalues λ and $\bar{\lambda}$, then we complexify and proceed exactly as in the distinct real case. More precisely we take $\bar{P}$ to have the form

$$\bar{P}(x+iy, x-iy) = \sum_{n=0}\sum_{m=0} v_{mn}(x+iy)^m\,(x-iy)^n$$

  with $v_{mn} \in \mathbb{C}^3$, and impose that $\bar{P}$ solves the invariance equation

$$f[\bar{P}(z_1, z_2)] = \bar{P}(\lambda z_1, \bar{\lambda} z_2).$$

  Proceeding as in the case of two distinct real eigenvalues we see that in this case the coefficients still solve the homological equation given by Equation (3.8) with $\lambda_1 = \lambda$ and $\lambda_2 = \bar{\lambda}$. The resulting complex coefficients have that $v_{(m,n)} = \overline{v_{(n,m)}}$, so that $P(x, y) = \bar{P}(x+iy, x-iy)$ is a real valued function. Then image(P) is again a (real) local stable manifold of p. A more thorough discussion of the complex conjugate case is found in [40].

- Note that the homological equation for the power series coefficients of the two dimensional stable/unstable parameterization has the form

$$[Df(p_0) - \lambda_1^m \lambda_2^n I]v_{mn} = \begin{pmatrix} -s_{mn} \\ 0 \\ 0 \end{pmatrix},$$

  which is analogous to the one dimensional result. Then the coefficients of the formal series exist uniquely for all m, n with $m + n \geq 2$, so long as the following *non-resonance* conditions is satisfied;

$$\lambda_1^m \lambda_2^n \neq \lambda_i \tag{3.9}$$

  for $i = 1, 2$.

  Let $\mu_- = \min(|\lambda_1|, |\lambda_2|)$ and $\mu_+ = \max(|\lambda_1|, |\lambda_2|)$. Then it is sufficient to check the non-resonance condition given by Equation (3.9) for each pair $(m, n) \in \mathbb{N}^2$ having

$$2 \leq m + n \leq \frac{\ln(\mu_-)}{\ln(\mu_+)}, \tag{3.10}$$

  as $m + n > \ln(\mu_-)/\ln(\mu_+)$ implies that

$$|\lambda_1|^m |\lambda_2|^n \leq (\mu_+)^{m+n} \leq \mu_- \tag{3.11}$$

  Then the non-resonance conditions given by Equation (3.9) reduce to a finite number of conditions. In practice we check the non-resonance conditions using rigorous interval arithmetic for each m, n given by Inequality (3.10). If we can confirm all of these conditions, then Inequality (3.11) implies there are no resonances at higher order.

- In fact the situation just describe is quite general. If $P : B \subset \mathbb{R}^k \to \mathbb{R}^n$ parameterizes a k dimensional (stable or unstable) invariant manifold of $f : \mathbb{R}^n \to \mathbb{R}^n$ and, using the notation of Section 3, we suppose that

$$P(\theta) = \sum_{|\alpha|>0} a_\alpha \theta^\alpha,$$

then a formal computation shows that the $|\alpha| \geq 2$ coefficients of the parameterization P satisfy the homological equation

$$[Df(p_0) - \Lambda^\alpha I]a_\alpha = s(\alpha') \tag{3.12}$$

where

$$\Lambda^\alpha = \lambda_1^{\alpha_1} \cdot \ldots \cdot \lambda_k^{\alpha_k} \in \mathbb{C},$$

s depends only on coefficients α' with $|\alpha'| < |\alpha|$, and the form of the function s depends only on the form of the nonlinearity of the function f (this formal computation is discussed in general in [9]). The coefficients a_α are then formally well defined as long as there are no resonances of the form

$$\lambda_1^{\alpha_1} \cdot \ldots \cdot \lambda_k^{\alpha_k} = \lambda_i$$

for any $1 \leq i \leq k$ and any $|\alpha| \geq 2$. In precise analogy with Inequalities 3.10 and 3.11 of the previous remark it is sufficient to check that there are no resonances for each

$$2 \leq |\alpha| \leq \frac{\ln(\mu_-)}{\mu_+}.$$

Again, this gives a finite number of conditions which can be checked rigorously using interval arithmetic. Then we can use Equation (3.12) to compute the manifold coefficients of stable and unstable manifolds of any dimension. In particular we use Equation (3.12) to compute the coefficients of the the two through ten dimensional manifolds of the delayed Hénon mapping in Section 3.3, as well as the four dimensional manifolds for the coupled Lomelí maps in Section 6.

3.3. Performance of Numerical Computation of the Parameterization Coefficients. In this section we work with the Delayed Hénon map described in Section 2.1. All computations are carried out using the *IntLab* implementation of interval arithmetic in MatLab. The IntLab package is equipped with subroutines for computing rigorous interval enclosures of the usual elementary functions, eigenvalues and eigenvectors of $n \times n$ matrices, and solutions of linear systems of equations. See [47] for complete details.

We compute the coefficients of the parameterization of the $n-1$ dimensional stable manifold at p_1 in dimensions $n = 3$ through $n = 11$ to various orders for $a = 1.6$ and $b = 0.1$. We obtain an interval enclosure of $x_1 \subset B(0.557857598881097, 2.221e-16)$ for the fixed point $p_1 = (x_1, \ldots, x_1)$.

First we consider the cost of computing parameterizations of the two dimensional stable manifold with varying polynomial order. We obtain interval enclosures of the stable eigenvalues

$$\lambda_s^1 \subset B(-0.25570156572582, 2.221e-16) \qquad \text{and} \qquad \lambda_s^2 \subset B(0.22314485443973, 1.388e-16).$$

and eigenvectors

$$\xi_s^1 \subset B\left(\begin{bmatrix} -0.06321850901795 \\ 0.24723551785264 \\ -0.96689090327176 \end{bmatrix}, 1.67e-16\right)$$

and

$$\xi_s^2 \subset B\left(\begin{bmatrix} 0.04854109103645 \\ 0.21753175155361 \\ 0.97484547470201 \end{bmatrix}, 1.67e-16\right)$$

Order	Number Non-Zero Coeff	Comp Time	Largest Interval Rad
2	6	0.064 sec	$3.61e-16$
3	10	0.143 sec	$3.61e-16$
4	15	0.257 sec	$3.61e-16$
5	21	0.396 sec	$3.61e-16$
10	66	1.41 sec	$3.61e-16$
15	136	3.80 sec	$3.61e-16$
20	231	8.35 sec	$3.61e-16$
30	496	32.01 sec	$3.61e-16$
60	1756	395.51 sec	$3.61e-16$

Table 3.1

Coefficient Computation Performance: Two-Dimensional Manifold; Three Dimensional Phase Space.

Phase Space Dim	Number Non-Zero Coeff	Comp Time	Largest Interval Rad
4 (3-D manifold)	20	0.478 sec	$4.11e-16$
5 (4-D manifold)	35	0.555 sec	$4.61e-16$
6 (5-D manifold)	56	0.820 sec	$5.46e-16$
7 (6-D manifold)	84	1.37 sec	$5.88e-16$
8 (7-D manifold)	120	3.43 sec	$6.98e-16$
9 (8-D manifold)	165	10.92 sec	$6.96e-16$
10 (9-D manifold)	220	52.72 sec	$9.11e-16$
11 (10-D manifold)	286	292.83 sec	$6.95e-16$

Table 3.2

Coefficient Computation Performance: Third order approximation of co-dimension one manifold in n-dimensional phase space.

Table 3.3 reports the performance data for computations with orders between $N = 2$ and $N = 60$. Each coefficient is a vector in $\mathbb{R}^3$ (the solution of the homological equation, which is a 3×3 linear system) so each non-zero coefficient consists of three intervals. Also given are the resulting computation times and the size of the largest containment interval of any coefficient.

We also compute the parameterization to third order for phase space dimensions 4 through 11 (manifold dimensions 3 through 10). The results are given in Table 3.3. Each increase in dimension leads to an increase in computation time of roughly a factor of four. The interval enclosure radii are related to the enclosure radii of the eigenvalues and eigenvectors, which get more difficult to enclose as the dimension increases. In every case all eigenvalues and eigenvectors are enclosed in balls with radii of no more than 5×10^{-16}.

3.4. Numerical Radius of Validity for Formal Solutions. Suppose that we have recursively solved the homological equations for the parameterization of a k dimensional (stable or unstable) manifold up to a fixed finite order N. Then we have a polynomial approximation

$$P_N(\theta) = \sum_{0 \leq |\alpha| \leq N} a_\alpha \theta^\alpha$$

to the true parameterization P. While any truncated approximation P_N is entire (as P_N is a polynomial), we do not expect that P_N is a good approximation to P for all θ. Instead, we would like to determine a fixed domain on which the approximation is “good”. The following definition makes this precise;

Definition 3.4. Let $\epsilon > 0$ be a prescribed tolerance, $\nu > 0$, and $B = B(0, \nu) \subset \mathbb{R}^k$. We call the number ν *an ϵ-numerical radius of validity* for the approximation P_N if

$$\text{Error}_\nu(P_N) \equiv \sup_{\theta \in B} \|f[P_N(\theta)] - P_N(\Lambda\,\theta)\| \leq \epsilon. \tag{3.13}$$

Remark 3.5.

- In practice, numerical experimentation is enough to select a good ν. Numerical examples and algorithm performance information for local manifolds computations for the Lomelí map can be found in Section 5 and Appendix A of [40]
- We have the usefull bound

$$\text{Error}_\nu(P_N) \leq \sum_{0 \leq |\alpha|} |C_\alpha - D_\alpha| \nu^{|\alpha|} \tag{3.14}$$

  where C_α, D_α are the power series coefficients of $f[P_N]$ and $P_N(\Lambda\,\theta)$ respectively. (The inequality is due to the maximum modulus principle). When f is a polynomial, all but finitely many of A_α, and B_α are zero. Then the sum is finite and Equation (3.5) is easy to rigorously bound numerically using interval arithmetic.
- Theorem 4.1 shows that under certain conditions which are easy to validate numerically, we actually have $\|P - P_N\|_\nu \leq C\epsilon$ where C is an explicitly known constant. This provides a mathematically rigorous *a-posteriori* bound on the truncation error made in approximating P by P_N.

4. A-Posteriori Validation of the Formal Series.

In this section we prove an *a-posteriori* validation theorem for parameterizations of stable and unstable manifolds for discrete time dynamical systems. From a theoretical view it is preferable to work with analytic functions defined on $\mathbb{C}^n$. For the sake of readability we re-state our assumptions.

A1 Let $p \in \mathbb{C}^n$, $\rho > 0$ and assume that that $f : B(p, \rho) \subset \mathbb{C}^n \to \mathbb{C}^n$ is a bounded analytic function, so that there is $K_0 > 0$ so that

$$\|f\|_\rho \leq K_0.$$

A2 Assume that $Df(p)$ is non-singular, diagonalizble, and hyperbolic. Let $\{\lambda_1^s, \ldots, \lambda_{n_s}^s\}$ and $\{\xi_1^2, \ldots, \xi_{n_s}^s\}$ denote the stable eigenvalues (which are distinct as $Df(p)$ is diagonalizable) and a choice of stable eigenvectors respectively. Let Λ denote the $n_s \times n_s$ diagonal matrix of stable eigenvalues and $Q_0 = [\xi_1^s|\ldots|\xi_{n_s}^s]$ denote the matrix whose columns are the stable eigenvectors.

A3 Assume that $P_N : B(0, \nu) \subset \mathbb{C}^{n_s} \to \mathbb{C}^n$ is an N-th order polynomial, with $N \geq 2$, which for each $\theta \in B(0, \nu)$ solves the equation

$$f[P_N(\theta)] = P_N(\Lambda\theta)$$

exactly to N-th order (in the sense that the power series coefficients of the function on the left are equal to the power series coefficients of the function on the right to N-th order).

Then we have the following definition.

Definition 4.1. [Validation values for discrete dynamical systems] The collection of positive constants ν, ϵ_{tol}, C_1, C_2, K_1, ρ, ρ', μ_* and μ^* are validation values for P_N if

1. $\|f \circ P_N - P_N \circ \Lambda\|_{\Sigma,\nu} \leq \epsilon_{\text{tol}}$;
2. $\|P_N\|_{\Sigma,\nu} \leq \rho' < \rho$;
3. $0 < \mu_* \leq \min_{1 \leq i \leq n_s} |\lambda_i^s| \leq \max_{1 \leq i \leq n_s} |\lambda_i^s| \leq \mu^* < 1$;

4.
$$\|Df[P_n]^{-1}\|_{\Sigma,\nu} \leq C_1\mu_*^{-1} + C_2(\nu);$$

where, as we will see in the proof, we take C_1 to be any constant with

$$\|Q_0\|\|Q_0^{-1}\| \leq C_1,$$

and C_2 to be any bound on the theta dependent terms of $Df[P_N(\theta)]^{-1}$ on B_ν.

5.
$$\max_{\substack{\beta \in \mathbb{Z}^n \\ |\beta| = 2}} \max_{1\leq j\leq n} \|\partial^\beta f_j\|_\rho \leq K_1(\rho).$$

The bounds in the validation theorem are improved if we take into account only the of non-zero second partials of f. Then we will define

$$N_f = \max_{1\leq j\leq n} \#\{\beta \in \mathbb{Z}^n : |\beta| = 2 \;\text{ and }\; \partial^\beta f_j \neq 0\}, \tag{4.1}$$

and of course have that $N_f \leq n^2$. However for a given map N_f may be smaller than this.

THEOREM 4.1 (A-posteriori manifold validation). *Given validation values ν, ϵ_{tol} , K_1, C_1, C_2, ρ, ρ', μ_* and μ^*, assume that N and δ satisfy the three inequalities*

$$N + 1 > \frac{\ln(\mu_*) - \ln(C_1 + \mu_* C_2)}{\ln(\mu^*)}; \tag{4.2}$$

$$\delta < \min\left(\frac{[\mu_* - (C_1 + \mu_* C_2)(\mu^*)^N]}{2ne\pi N_f(C_1 + \mu_* C_2)K_1}, (\rho - \rho')e^{-1}\right) \tag{4.3}$$

$$\delta > \frac{2(C_1 + \mu_* C_2)\epsilon_{tol}}{\mu_* - (C_1 + \mu_* C_2)(\mu^*)^N} \tag{4.4}$$

Then there is a unique parameterization function $P : B(0,\nu) \subset \mathbb{C}^{n_s} \to \mathbb{C}^n$ solving Equation 3.1. Additionally, the truncation error is bounded by

$$\|P - P_N\|_\nu \leq \delta$$

and the parameterization coefficients $a_\alpha \in \mathbb{C}^n$ decay as

$$|a_\alpha| \leq \frac{\delta}{\nu^{|\alpha|}} \qquad \text{for } \; |\alpha| > N.$$

REMARK 4.2. [The Resonance Condition] While the meanings of the conditions given by Equations 4.2, 4.3, and 4.4 will become clear in the Sections 4.2 and 4.3, when we discuss the proof of Theorem 4.1, it is appropriate to make a small remark about Equation 4.2 presently. Note that the right hand side of Equation 4.2 is the natural logarithm of the ratio of the smallest to the largest eigenvalue of $Df(p)$ (the spectral gap) minus a correction term which reflects the nonlinearity of f at p. The condition given by Equation 4.2 guarantees that N is so large enough that there is no possibility of resonances in the coefficients of the remainder $P - P_N$.

4.1. Analytic Preliminaries. If $x \in \mathbb{R}$, then we use $|x|$ to denote the usual absolute value. Similarly, for $z = a + ib \in \mathbb{C}$ we use the usual "Euclidian" norm $|z| = \sqrt{a^2 + b^2}$. We endow $\mathbb{R}^n$ and $\mathbb{C}^n$ with the so called sup or infinity norms generated by the real or complex absolute value functions, so that for $x = (x_1, \ldots, x_n) \in \mathbb{R}^n$ and $z = (z_1, \ldots, z_n) \in \mathbb{C}^n$ we have

$$|x| = \max_{1\leq i\leq n} |x_i|, \quad \text{and} \quad |z| = \max_{1\leq i\leq n} |z_i|$$

where in each case the $|\cdot|$ on the right is either the absolute value for $\mathbb{R}$ or $\mathbb{C}$, and the sup is taken over components. These norms are well suited for numerical work, as they are easy to evaluate and introduce no rounding errors.

For fixed $\hat{z} \in \mathbb{C}^m$ and $\nu > 0$ let $B_\nu(\hat{z}) \subset \mathbb{C}^m$ be the ball (or *poly-disk*) of radius ν about $\hat{z}$ generated by the sup-norm, so

$$B_\nu(\hat{z}) \equiv \{(h_1, \ldots, h_m) \in \mathbb{C}^m \;:\; |\hat{z}_i - h_i| < \nu \;\text{ for each }\; 1 \leq i \leq m\}.$$

A function $g : B_\nu(\hat{z}) \subset \mathbb{C}^m \to \mathbb{C}$ is analytic on the poly-disk $B_\nu(\hat{z})$ if g has a power series expansion

$$g(z) = \sum_{|\alpha| \geq 0} a_\alpha (\hat{z} - z)^\alpha \qquad \alpha \in \mathbb{N}^m \qquad a_\alpha \in \mathbb{C},$$

which converges for all $z \in B_\nu(\hat{z})$. Here we use the usual *multi-index* notation, so that if $\alpha = (\alpha_1, \ldots, \alpha_m) \in \mathbb{N}^m$ and $z \in \mathbb{C}^m$ then $|\alpha| = \alpha_1 + \ldots + \alpha_m$ and $z^\alpha = z_1^{\alpha_1} \cdot \ldots \cdot z_m^{\alpha_m}$.

We say that $f : B_\nu(\hat{z}) \subset \mathbb{C}^m \to \mathbb{C}^n$ is analytic on $B_\nu(\hat{z})$ if $f = (f_1, \ldots, f_n)$ and each $f_j : B_\nu(0) \subset \mathbb{C}^m \to \mathbb{C}$, $1 \leq j \leq n$ is analytic in the sense just described. Such an f can also be expressed in power series form as

$$f(z) = \sum_{|\beta| > 0} b_\beta (\hat{z} - z)^\beta \qquad \beta \in \mathbb{N}^m \qquad b_\beta \in \mathbb{C}^n$$

which converges for all $z \in B_\nu(\hat{z})$. The space of bounded analytic functions on $B_\nu(\hat{z})$ forms a Banach space under the norm

$$\|f\|_{B_\nu(\hat{z}), \Sigma} \equiv \sum_{|\alpha| \geq 0} |b_\alpha| \nu^{|\alpha|}.$$

Of course the bounded analytic functions are also a Banach space under the usual C^0 norm, and that the two norms are related by

$$\|f\|_{B_\nu(\hat{z})} \equiv \max_{1 \leq j \leq n} \max_{1 \leq i \leq m} \sup_{|z_i - \hat{z}_i| \leq \nu} |f_j(z_1, \ldots, z_m)| \leq \|f\|_{B_\nu(\hat{z}), \Sigma}.$$

In theoretical arguments we often use the C^0 norm $\|\cdot\|_{B_\nu(\hat{z})}$, while in numerical applications it is often convenient to use the *sigma-norm* $\|\cdot\|_{B_\nu(\hat{z}), \Sigma}$ in conjunction with the above inequality. Also, by the maximum modulus principle we have that if f is uniformly bounded and analytic on (the open set) $B_\nu(\hat{z})$, then

$$\|f\|_{B_\nu(\hat{z})} = \max_{1 \leq j \leq n} \sup_{|z_i - \hat{z}_i| = \nu} |f_j(z_1, \ldots, z_m)|,$$

so that f is in fact bounded on the closed ball. It follows that f is continuous on $\partial B_\nu(\hat{z})$. If the ball in question is centered at the origin, i.e. is a ball of the form $B_\nu(0)$ then we sometimes use the notation $\|\cdot\|_{\nu, \Sigma}$ and $\|\cdot\|_\nu$ for $\|\cdot\|_{B_\nu(0), \Sigma}$ and $\|\cdot\|_{B_\nu(0)}$ respectively.

Suppose that A is an $n \times m$-matrix with entries $a_{ij} \in \mathbb{C}$. Then when we consider a A as a linear operator $A : \mathbb{C}^m \to \mathbb{C}^n$ we employ the usual operator norm

$$\|A\|_M = \sup_{|\eta| = 1} |A \cdot \eta|,$$

where $\eta \in \mathbb{C}^m$ and $\cdot$ is matrix-vector multiplication. Since $|\cdot|$ is the sup-norm on components we have that

$$\|A\|_M \leq \sup_{1 \leq i \leq n} \sum_{j=1}^{m} |a_{ij}| \leq m \sup_{1 \leq i \leq n} \sup_{1 \leq j \leq m} |a_{ij}|. \tag{4.5}$$

Given a fixed $\hat{z} \in \mathbb{C}^k$ and $\nu > 0$, suppose that $g : B_\nu(\hat{z}) \subset \mathbb{C}^k \to \mathbb{C}^m$ is an analytic function and suppose that the entries of the $n \times m$ matrix A are themselves analytic functions $a_{ij} : B_\nu(\hat{z}) \subset \mathbb{C}^k \to \mathbb{C}$. We can define the norm of the non-constant matrix A to be

$$\|A\|_{M,B_\nu(\hat{z})} \equiv \max_{1\leq i\leq n} \sum_{j=1}^{m} \|a_{ij}\|_{B_\nu(\hat{z})}$$

Then the non-constant matrix vector product $A \cdot g : B_\nu(\hat{z}) \subset \mathbb{C}^k \to \mathbb{C}^n$ is an analytic function and we have the bounds

$$\|A \cdot g\|_{B_\nu(\hat{z})} \leq \|A\|_{M,B_\nu(\hat{z})} \|g\|_{B_\nu(\hat{z})} \leq m \|g\|_{B_\nu(\hat{z}),\Sigma} \max_{1\leq i\leq n} \max_{1\leq j\leq m} \|a_{ij}\|_{B_\nu(\hat{z}),\Sigma},$$

the last bound being particularly useful for numerical applications.

The family of analytic functions which are zero to N-th order play an important in the arguments to follow. We say that $h : B_\nu(0) \subset \mathbb{C}^m \to \mathbb{C}^n$ is an *analytic N-tail* if h is analytic on $B_\nu(0)$ and

$$h(0) = 0, \quad Dh(0) = 0, \quad \ldots \quad D^\alpha h(0) = 0, \qquad \text{for} \qquad |\alpha| \leq N.$$

Then an analytic N-tail h always has power series representation

$$h(z) = \sum_{|\beta|>N} b_\beta z^\beta \qquad \beta \in \mathbb{N}^m \qquad b_\beta \in \mathbb{C}^n$$

converging for each $|z| < \nu$. With m, n, and $\nu > 0$ fixed we define $\mathbb{H}_N$ to be the set of bounded analytic N-tials on $B_\nu(0) \subset \mathbb{C}^m$ taking values in $\mathbb{C}^n$ (n, m, and ν will always be clear from context).

We use freely the following well known facts about analytic functions and N-tails.

LEMMA 4.2.

1. *If $\hat{z} \in \mathbb{C}^m$, $\nu > 0$, $f : B_\nu(\hat{z}) \to \mathbb{C}^n$ is analytic and $\|f\|_\nu \leq M$, then one has for each $\beta \in \mathbb{N}^m$ the Cauchy Estimates*
$$|b_\beta| \leq \frac{M}{\nu^{|\beta|}}.$$
2. *Let h be a bounded analytic N-tail on $B_\nu(0) \subset \mathbb{C}^m$ and $\lambda_1, \ldots, \lambda_m \in \mathbb{C}$be non-zero complex numbers with $0 < |\lambda_j| < 1$, for $1 \leq j \leq m$. Suppose that Λ is the $m \times m$ matrix with λ_j in the j-th diagonal entry and zeros in the non-diagonal entries, and that $0 < \mu^* \equiv \sup_j |\lambda_j| < 1$. Then $h \circ \Lambda$ is a bounded analytic N-tail on $B_\nu(0)$ and*
$$\|h \circ \Lambda\|_\nu \leq (\mu^*)^{N+1} \|h\|_\nu \ .$$
3. *If $g : B_\nu(0) \subset \mathbb{C}^m \to \mathbb{C}$ is analytic and $\hat{z} \in \mathbb{C}^m$ has $|\hat{z}| < \nu$, then g is analytic on the poly-disk $B_s(\hat{z})$, $s = \nu - |\hat{z}|$ and for any $\eta \in B_s(\hat{z})$, g can be expanded as*
$$g(\hat{z} + \eta) = g(\hat{z}) + Dg(\hat{z}) \cdot \eta + R_{\hat{z}}(\eta)$$
where
$$\|R_{\hat{z}}\|_s \leq N_g K s^2.$$
Here N_g is the number of non-zero second partial derivatives of of g at $\hat{z}$ (so $N_g \leq m^2$) and K is any constant having
$$\sup_{|\beta|=2} \|\partial_\beta g\|_s \leq K.$$
If f is analytic on $B_\nu(0) \subset \mathbb{C}^m$ with values in $\mathbb{C}^n$ then the result can be applied to f component by component.
4. *If $f : B_\nu(\hat{z}) \subset \mathbb{C}^m \to \mathbb{C}^n$ is analytic and $z_1, z_2 \in B_\nu(\hat{z})$ then*
$$|f(z_1) - f(z_2)| \leq \|Df\|_{M,B_\nu(\hat{z})} |z_1 - z_2|.$$

For (1) see any standard text on complex analysis (for example [1]). The elementary proof of (2) is in [6]. (3) is the Lagrange form of the Taylor remainder theorem (also for example in [1]), while (4) is the mean value theorem combined with our norm definitions.

In the following let X be a Banach space, $\mathbb{L}(X)$ be the Banach space of all bounded linear operators on X, and $A \in \mathbb{L}(X)$. Then

$$\|A\|_{\mathbb{L}(X)} \equiv \sup_{x \in X, \|x\|_X = 1} \|Ax\|_X = M < \infty.$$

We make use of the following standard theorems from non-linear analysis.

- **Contraction Mapping Theorem** Let $x \in X$,

$$B_r(x) = \{y \in X \,:\, \|x - y\|_X \leq r\},$$

  and suppose that $\Phi : B_r(x) \to B_r(x)$ is continuous. If in addition there is a $0 < \kappa < 1$ so that for any $x_1, x_2 \in B_r(x)$ we have

$$\|\Phi(x_1) - \Phi(x_2)\|_X \leq \kappa \|x_1 - x_2\|_X$$

  then there is a unique $\hat{x} \in B_r(x)$ so that $\Phi(\hat{x}) = \hat{x}$.

- **Neumann Series** If $I : X \to X$ is the identity map and $A : X \to X$ is a bounded linear operator with $\|A\|_{\mathbb{L}(X)} \leq 1$ then $I - A$ is boundedly invertible and

$$[I - A]^{-1} = \sum_{k=0}^{\infty} A^k,$$

  from which it follows that

$$\|(I - A)^{-1}\|_{\mathbb{L}(X)} \leq \sum_{k=0}^{\infty} \|A\|_{\mathbb{L}(X)}^k \leq \frac{1}{1 - M}.$$

Our "analytic homoclinic shadowing theorem" (Theorem 5.1) is based on the Newton-Kantorovich Theorem [30, 31].

THEOREM 4.3 (Newton-Kantorovich Method). *Let X, Y be Bancah spaces and $F : X \to Y$ be a differentiable mapping. Assume that there as an $\hat{x} \in X$ and an $r > 0$ such that*

(i) $DF(\hat{x})$ has bounded inverse, and

(ii) $\|DF(x) - DF(y)\|_{B(X,Y)} \leq \kappa \|x - y\|$ for all $x, y \in B_r(\hat{x})$.

If

(I)

$$\epsilon_{NK} \geq \|DF(\hat{x})^{-1}\, F(\hat{x})\|_X,$$

(II)

$$\epsilon_{NK} \leq \frac{r}{2},$$

and

(III)

$$4\epsilon_{NK}\, \kappa\, \|DF(\hat{x})^{-1}\|_{B(X,Y)} \leq 1,$$

then the equation

$$F(x) = 0$$

has a unique solution in $B(r, \hat{x})$.

For an english language exposition of the proof, see also [45]

Finally we require the following bounds for derivatives of analytic functions. The Lemma 4.3 tells us how to bound the derivatives of an analytic function in terms of a bound on the function itself, *so long as we are willing to give up some portion of the domain of analyticity.* The estimates are considered "standard" in KAM theory. (For example they are left as an exercise in [35], and are similar to the bounds for Fourier series found in Section 2.5.7 of [16]. Similar, but less optimal, estimates are in [55, 6]) We include a brief proof in order to obtain explicitly the constants, as we must apply the bounds in the context of computer assisted arguments. Our aim is to give an elementary and brief computation and we note that our constants are obviously not sharp. On the other hand we do take care to obtain the optimal order in the *loss of domain parameter* σ.

LEMMA 4.3 (Cauchy Bounds). *Suppose that* $f : B_\nu(0) \subset \mathbb{C}^m \to \mathbb{C}^n$ *is bounded and analytic. Then for any* $0 < \sigma \leq 1$ *we have that*

$$\|\partial_i f\|_{\nu e^{-\sigma}} \leq \frac{2\pi}{\nu\sigma}\|f\|_\nu \quad \text{so that} \quad \|Df\|_{\nu e^{-\sigma}} \leq \frac{2\pi m}{\nu\sigma}\|f\|_\nu, \tag{4.6}$$

as well as

$$\|\partial_i\partial_j f\|_{\nu e^{-\sigma}} \leq \frac{4\pi^2}{\nu^2\sigma^2}\|f\|_\nu \quad \text{and} \quad \|D^2 f\|_{\nu e^{-\sigma}} \leq \frac{4\pi^2 m^2}{\nu^2\sigma^2}\|f\|_\nu. \tag{4.7}$$

Proof: Consider first the one dimensional case, where $\nu > 0$ and $f : B_\nu(0) \subset \mathbb{C} \to \mathbb{C}$ is analytic. Let $0 < \sigma \leq 1$. Then using Cauchy's formula [1] we have that for any $z \in B_{\nu e^{-\sigma}}(0)$

$$f'(z) = \frac{1}{2\pi i}\int_{|\xi|=\nu} \frac{f(\xi)}{(\xi - z)^2}\, d\xi.$$

Note that the denominator is bounded precisely because $|z| \leq \nu e^{-\sigma}$, i.e. because we are taking z in a reduced domain. (Choosing to reduce the domain by an amount exponential in σ gives the optimal $1/\sigma$ dependance in the final estimate, as will be seen in the proof). We parameterize the path $|\xi| = \nu$ by $\xi(\theta) = \nu e^{i\theta}$ and take norms to obtain

$$\begin{aligned}
|f'(z)| &= \frac{1}{2\pi}\left|\int_0^{2\pi} \frac{f[\nu e^{i\theta}]i\nu e^{i\theta}}{(\nu e^{i\theta} - z)^2}\, d\theta\right| \\
&\leq \frac{1}{2\pi}\int_0^{2\pi} \frac{\nu\|f\|_\nu}{|\nu e^{i\theta} - z|^2}\, d\theta \\
&\leq \frac{\|f\|_\nu}{2\pi\nu}\int_0^{2\pi} \frac{1}{|e^{i\theta} - e^{-\sigma}|^2}\, d\theta,
\end{aligned} \tag{4.8}$$

where the last inequality is due to the fact that $|z| \leq \nu e^{-\sigma}$, so that the denominator is minimized when $|z| = \nu e^{-\sigma}$. Since the integrand is radially symmetric once we take the norm of f, we are free to take $z = \nu e^{-\sigma}$, and then factor a ν^2 out of the denominator of the integrand.

Noting that $e^\sigma \geq 1 + \sigma$ for all real σ, we have that $\sigma/(1+\sigma) \leq 1 - e^{-\sigma}$ for all $\sigma > -1$. Then for $0 < \sigma \leq 1$ we have

$$\sigma/2 \leq \frac{\sigma}{1+\sigma} \leq 1 - e^{-\sigma} \leq |e^{i\theta} - e^{-\sigma}|, \tag{4.9}$$

for all $0 \leq \theta \leq 2\pi$. Naive application of Eq (4.9) to Eq (4.8) would yield $|f'(z)| \leq 4\|f\|_\nu/\sigma^2$. However a slightly more subtle argument yields an estimate which is only inverse proportional to σ. Eq (4.8) can be re-written as

$$\begin{aligned}
&\frac{\|f\|_\nu}{2\pi\nu}\int_0^{2\pi} \frac{1}{|e^{i\theta} - e^{-\sigma}|^2}\, d\theta \\
&= \frac{\|f\|_\nu}{2\pi\nu}\left(\int_{-\frac{\sigma}{2}}^{\frac{\sigma}{2}} \frac{1}{|e^{i\theta} - e^{-\sigma}|^2}\, d\theta + \int_{\frac{\sigma}{2}}^{2\pi - \frac{\sigma}{2}} \frac{1}{|e^{i\theta} - e^{-\sigma}|^2}\, d\theta\right)
\end{aligned} \tag{4.10}$$

For the first of the integrals on the right in Eq (4.10) we exploit Eq (4.9) to obtian

$$\int_{-\frac{\sigma}{2}}^{\frac{\sigma}{2}} \frac{1}{|e^{i\theta} - e^{-\sigma}|^2} \, d\theta \leq \int_{-\frac{\sigma}{2}}^{\frac{\sigma}{2}} \frac{1}{|\frac{\sigma}{2}|^2} \, d\theta \leq \frac{4}{\sigma}. \tag{4.11}$$

On the other hand, since $|e^{i\theta} - e^{-\sigma}| \geq \sin\theta \geq 2\theta/\pi$ for $0 \leq \theta \leq \pi/4$, the second integral on the right in Eq (4.10) satisfies the bound

$$\int_{\frac{\sigma}{2}}^{2\pi - \frac{\sigma}{2}} \frac{1}{|e^{i\theta} - e^{-\sigma}|^2} \, d\theta \leq 4 \int_{\frac{\sigma}{2}}^{\frac{\pi}{2}} \frac{\pi^2}{4\theta^2} \leq \frac{2\pi^2}{\sigma} \tag{4.12}$$

Racalling that $z \in B_{\nu e^{-\sigma}}(0)$ we note that Eq (4.11) and Eq (4.12) are uniform in z and combine them with Eq (4.10) to obtain

$$\|f'\|_{\nu e^{-\sigma}} \leq \frac{1}{2\pi\nu} \left(\frac{4}{\sigma} + \frac{2\pi^2}{\sigma} \right) \|f\|_\nu \leq \frac{2\pi}{\nu\sigma} \|f\|_\nu. \tag{4.13}$$

If $f : B_\nu(0) \subset \mathbb{C}^m \to \mathbb{C}^n$ then each $f_k(z_1, \ldots, z_i, \ldots, z_m)$, $1 \leq i \leq m$, $1 \leq k \leq n$ is analytic in the i-th variable (with the other variables held fixed), so that we obtain

$$\left| \frac{\partial}{\partial z_i} f_k(z) \right| \leq \frac{2\pi}{\nu\sigma} \|f\|_\nu,$$

for any $|z| \leq \nu e^{-\sigma}$ by applying the same argument to the Cauchy integral of $\partial/\partial z_i f_k(z)$. Since this is uniform in i, k and z we apply the estimate given by Equation (4.5) in order to obtian

$$\|Df\|_{\nu e^{-\sigma}} \leq \frac{2\pi m}{\nu\sigma} \|f\|_\nu,$$

as desired. The same estimates can be applied to the Cauchy type integral

$$\frac{\partial}{\partial z_i} \frac{\partial}{\partial z_j} f(z) = \frac{1}{(2\pi i)^2} \int_{|\xi_i| = \nu} \int_{|\xi_j| = \nu} \frac{f(z_1, \ldots, \xi_i, \ldots, \xi_j, \ldots, z_m)}{(\xi_i - z_i)^2 \, (\xi_j - z_j)^2} \, d\xi_i \, d\xi_j$$

to obtain in a similar fashion that

$$\|D^2 f\|_{\nu e^{-\sigma}} \leq \frac{4\pi^2 m^2}{\nu^2 \sigma^2} \|f\|_\nu,$$

as desired.

□

4.2. Proof of the Validation Theorem. We seek an analytic N-tail $h : B_\nu \to \mathbb{R}^n$ so that $P = P_N + h$ and having $\|h\|_\nu \leq \delta$ as small as possible (note that δ bounds the truncation error in the approximation P_N). The key observation is that h itself solves a certain functional equation. To see this let $P = P_N + h$ so that Equation 3.1 becomes

$$f[P_N + h] = [P_N + h](\Lambda).$$

Since f is analytic in $B_\rho \subset \mathbb{R}^n$, and since $\|P_N\|_\nu \leq \rho' \leq \rho$, f has a Taylor expansion about $P_N(\theta)$ for each $\theta \in B_s$. Then let $\theta \in B_s$ so that

$$f[P_N(\theta) + h(\theta)] = f[P_N(\theta)] + Df[P_N(\theta)] \, h(\theta) + R_{P_N(\theta)}(h(\theta)), \tag{4.14}$$

where for any $|z| \leq \rho'$, R_z is the Taylor remainder of f expanded at z. Again, since f is analytic on $\rho > \rho'$ we have that $R_z(\eta)$ is analytic on a disk of radius $s = \rho - \rho'$. Let

$$E(\theta) = f[P_N(\theta)] - P_N(\Lambda\theta) \tag{4.15}$$

and note that E is an analytic N-tail by the assumption that P_N solves Equation 3.1 exactly to N-th order. Then using Equations 4.14 and 4.15 in Equation 3.1 we have a new operator equation in terms of h

$$h[\Lambda\theta] - Df[P_N(\theta)]h(\theta) = E(\theta) + R_{P_N}(h). \tag{4.16}$$

In order to re-write Equation 4.16 as a fixed point equaiton on $\mathbb{H}_N$, the Banach Space of all analytic N-tails from B into $\mathbb{C}^n$, consider the linear operator $\mathfrak{L} : \mathbb{H}_N \to \mathbb{H}_N$ defined by the left hand side of Equation 4.16. So for any $p, q \in \mathbb{H}_N$ we define $\mathfrak{L}[q]$ to be

$$\mathfrak{L}[q](\theta) = q[\Lambda\theta] - Df[P_N(\theta)]h(\theta),$$

and our first task is to study the equation $\mathfrak{L}[q] = p$. He have that

Lemma 4.4. *Let C_1, C_2, μ_* and μ^* be validation values as in Definition 4.1. Suppose that N satisfies the assumption given by Equation 4.2 of Theorem 4.1. Then the linear operator $\mathfrak{L}$ is boundedly invertible on H_N, so that for any $p \in H$ there exists a unique solution to the equation*

$$\mathfrak{L}[q] = p.$$

Moreover we have the bound

$$\|\mathfrak{L}^{-1}\| \le \frac{C_1 + \mu_* C_2}{\mu_* - (C_1 + \mu_* C_2)(\mu^*)^N}.$$

Using Lemma 4.4 we apply $\mathfrak{L}^{-1}$ to both sides of Equation 4.16 to see that if $P = P_N + h$ then

$$h = \mathfrak{L}^{-1}\left[E(\theta) + R_{P_N}[h(\theta)].\right]$$

Define the non-linear operator $\Phi : \mathbb{H}_N \to \mathbb{H}_N$ to be

$$\Phi(h) = \mathfrak{L}^{-1}\left[E(\theta) + R_{P_N}[h(\theta)]\right]. \tag{4.17}$$

The preceding discussion makes it clear that $P = P_N + h$ is an exact solution of Equation 3.1 if and only if h is a fixed point of Equation 4.17. What remains is to show that if the assumptions given by Equations 4.2, 4.3 and 4.4 are satisfied, then Φ admits a unique fixed point h. A natural strategy is to employ the Banach Contraction Mapping Theorem. In fact, as we will see in the next section, the assumptions given by Equations 4.3 and 4.4 are exactly the conditions which make Φ a local contraction near P_N.

Lemma 4.5. *Under the hypotheses of Theorem 4.1 Φ is a contraction on the ball $U_\delta = \{h \in \mathbb{H}_N : \|h\|_\nu \le \delta\}$. Hence there is a unique fixed point h of Φ on U_δ so that $P_N + h$ is an exact solution of Equation 3.1.*

Then Theorem 4.1 is true as soon as the lemmas are proved. Note that on an heuristic level, it is natural to expect that Φ is a contraction as E is a small constant (with respect to h), and R_{P_N} should depend "quadratically" on h.

4.3. Proofs of the Lemmas.

Now we complete the proof of Theorem 4.1 by providing the proofs of the lemmas.

Proof of Lemma 4.4: Let p and q be bounded analytic N-tails on B_ν and consider the equation

$$\mathfrak{L}[q](\theta) \equiv q[\Lambda\theta] - Df[P_N(\theta)]q(\theta) = p(\theta). \tag{4.18}$$

If we let $\bar{p}(\theta) \equiv -Df[P_N(\theta)]^{-1}p(\theta)$ then this is equivalent to

$$q(\theta) - Df[P_N(\theta)]^{-1}q(\Lambda\theta) = \bar{p}(\theta),$$

which upon defining the linear operator

$$A[q](\theta) \equiv Df[P_N(\theta)]^{-1} q(\Lambda\theta)$$

becomes

$$(I - A)[q](\theta) = \bar{p}(\theta).$$

Now consider the norm

$$\begin{aligned}
\|A\|_{\mathbb{H}_N} &\equiv \sup_{\|\eta\|_\nu = 1} \|A[\eta](\theta)\|_\nu \\
&= \sup_{\|\eta\|_\nu = 1} \|Df[P_N](\eta \circ \Lambda)\|_\nu \\
&\leq \sup_{\|\eta\|_\nu = 1} (C_1 \mu_*^{-1} + C_2)|\Lambda|^{N+1} \|\eta\|_\nu \\
&\leq \mu_*^{-1}(C_1 + \mu_* C_2)(\mu^*)^{N+1},
\end{aligned}$$

where we have used the bound from Equation 4.19 and Estimate 2 of Lemma 4.2. Then we apply the assumption given by Equation (4.2) of Theorem 4.1 and see that

$$\|A\|_{\mathbb{H}_N} \leq \frac{(C_1 + \mu_* C_2)(\mu^*)^{N+1}}{\mu_*} < 1.$$

It follows from the Neumann Theorem that $(I - A)$ is boundedly invertible, and that we have the bound

$$\|(I - A)^{-1}\|_{\mathbb{H}_N} \leq \sum_{i=0}^{\infty} \|A\|_{\mathbb{H}_N}^i = \frac{1}{1 - \frac{C_1(\mu^*)^{N+1}}{\mu_*}}.$$

From the bounded invertability of $(I - A)$ we obtain a unique solution to Equaiton 4.18 in the form

$$q(\theta) = (I - A)^{-1}[\bar{p}](\theta) = -(I - A)^{-1} Df[P_N(\theta)]^{-1} p(\theta).$$

Since p and q were arbitrary we have

$$\begin{aligned}
\|\mathfrak{L}^{-1}\|_{\mathbb{H}_N} &\leq \|(I - A)^{-1}\|_{\mathbb{H}_N} \|Df[P_N]^{-1}\|_{\Sigma,\nu} \\
&\leq \frac{1}{1 - \frac{(C_1 + \mu_* C_2)(\mu^*)^{N+1}}{\mu_*}} (\mu_*^{-1} C_1 + C_2) \\
&\leq \frac{C_1 + \mu_* C_2}{\mu_* - (C_1 + \mu_* C_2)(\mu^*)^{N+1}},
\end{aligned}$$

as desired.

□

Proof of Lemma 4.5: Since we hypothesized Equation 4.2, we can apply Lemma 4.4 and have that $\mathfrak{L}^{-1}$ is a well defined bounded linear operator. Then the operator

$$\Phi[h](\theta) \equiv \mathfrak{L}^{-1}\left[E(\theta) + R_{P_N(\theta)}[h](\theta)\right]$$

is well defined. To employ the Banach Fixed Point Theorem we must establish that when $U_\delta = \{h \in H_N : \|h\|_\nu \leq \delta\}$ is a δ-neighborhood in the space of analytic N-tails and δ satsfies the hypotheses of Theorem 4.1 and then

(i) Φ maps U_δ into itself.

(ii) there is a $0 < \kappa < 1$ so that for any $h_1, h_2 \in U_\delta$ one has $\|\Phi(h_1) - \Phi(h_2)\|_\nu \leq \kappa\|h_1 - h_2\|_\nu$.

In order to establish (i) we first note that for any $z, \eta \in \mathbb{C}^n$ with $|z| \leq \rho'$ and $|\eta| \leq s \equiv \rho - \rho'$ we have that

$$|R_z^j(\eta)| \leq N_f K_1 s^2$$

by straightforward application of the Lagrange Form of the Taylor Remainder to each of the $1 \leq j \leq n$ components of $R_z(\eta)$ (this estimate is carried out explicitly in [6] see Equaiton (75)). Then since $\|P_N\|_\nu \leq \|P_N\|_{\Sigma,\nu} \leq \rho'$ by by the definition of validation values (def 4.1) and $\delta < se^{-1} < s$ we have for each $\theta \in B_\nu$

$$|R_{P_N(\theta)}(h(\theta))|] \leq |R_z(h(\theta))| \leq \|R_z\|_\delta \leq \frac{\delta^2}{s^2}\|R_z\|_s \leq N_f K_1 \delta^2.$$

Then

$$\begin{aligned}
\|\Phi(h)\|_\nu &\leq \|\mathfrak{L}^{-1}\| \left(\|E\|_\nu + \|R_{P_N}(h)\|_\nu\right) \\
&\leq \frac{C_1 + \mu_* C_2}{\mu_* - (C_1 + \mu_* C_2)(\mu^*)^{N+1}} \left(\epsilon_{\text{tol}} + N_f K_1 \delta^2\right)
\end{aligned}$$

But

$$\frac{C_1 + \mu_* C_2}{\mu_* - (C_1 + \mu_* C_2)(\mu^*)^{N+1}} \epsilon_{\text{tol}} \leq \frac{\delta}{2}$$

and

$$\frac{C_1 + \mu_* C_2}{\mu_* - (C_1 + \mu_* C_2)(\mu^*)^{N+1}} N_f K_1 \delta^2 \leq \frac{\delta}{2},$$

as we see by applying the hypotheses given by Equations 4.3 and 4.4 respectively. Then Φ does in fact map into U_δ, as desired.

To establish (ii) we begin by considering the differential of the remainder term. Then let $\theta \in B_\nu$ and $z = P_N(\theta)$ and note that $|z| \leq \rho'$ (due to the definition of validation values, see Def (4.1)). Since $\delta < se^{-1} < s$ we choose a $0 < \sigma \leq 1$ and let $\omega = \delta/se^{-\sigma}$ so that for any and $h \in U_\delta$ we have the bound

$$\begin{aligned}
\|DR_z(h(\theta))\|_\delta &= \|DR_z \circ \omega\|_{se^{-\sigma}} \\
&\leq \omega \|DR_z\|_{se^{-\sigma}} \\
&\leq \frac{\delta}{se^{-\sigma}} \frac{2\pi n \sigma^{-1}}{s} \|R_z\|_s \\
&\leq \frac{2n\pi e^\sigma N_f K_1}{\sigma} \delta, \\
&\leq 2ne\pi N_f K_1 \delta.
\end{aligned}$$

Here we have used the Taylor Estimate of Lemma 4.2, the Cauchy Bounds of Estimate 4.3, the N-tail scaling estimate of Lemma 4.2, the fact that $\sigma^{-1}e^\sigma$ is minimized at $\sigma = 1$, and the assumption that that $\delta < e^{-1}s$.

Then for any $h_1, h_2 \in U_\delta$ we have

$$|R_z^j(h_1(\theta)) - R_z^j(h_2(\theta))| \leq 2ne\pi N_f K_1 \delta \|h_1 - h_2\|_\nu$$

by the mean value theorem. So

$$\begin{aligned}
\|\Phi(h_1) - \Phi(h_2)\|_\nu &= \left\|\mathfrak{L}^{-1}[E - R_{P_N}(h_1)] - \mathfrak{L}^{-1}[E - R_{P_N}(h_2)]\right\|_\nu \\
&= \|\mathfrak{L}^{-1}[R_{P_N}(h_1) - R_{P_N}(h_2)\|_\nu \\
&\leq \frac{C_1 + \mu_* C_2}{\mu_* - (C_1 + \mu_* C_2)(\mu^*)^{N+1}} 2ne\pi N_f K_1 \delta \|h_1 - h_2\|_\nu \\
&\leq \kappa \|h_1 - h_2\|_\nu,
\end{aligned}$$

where

$$\kappa \equiv \frac{2ne\pi N_f(C_1+\mu_* C_2)K_1}{[\mu_* - (C_1+\mu_* C_2)(\mu^*)^{N+1}]}\delta < 1,$$

as δ satisfies the hypothesis given by Equation (4.3) of Theorem (4.1).

□

4.4. The Bounds C_1 and C_2 when f is polynomial. In this section we describe how to obtain the bounds on the non-constant matrix $Df[P_N(\theta)]^{-1}$ required in the definition of validation values. We focus on the case where f is a polynomial. This is the only part of the validation argument that makes the polynomial assumption. We note that if f is a general analytic function then we can use the Taylor expansion of f to obtain that f is polynomial plus a remainder as small as we wish. The argument given here can be modified to work in this more general case as well. We do not pursue the details here.

By the inverse function theorem we have

$$Df[P_N(\theta)]^{-1} = Df^{-1}[f \circ P_N(\theta)],$$

which can be used to compute an analytic expression for $Df[P_N]^{-1}$ as long as f^{-1} is known explicitly. Then we let

$$Df(x)^{-1} = \sum_{|\beta|\geq 0}^{M-1} B_\beta x^\beta$$

where each B_β is an $n \times n$ matrix, and M is the order of f. Recall also that

$$P_N(\theta) = \sum_{0\leq|\alpha|\leq N} a_\alpha \theta^\alpha.$$

Then if $\bar{N} = N(M-1)$ we have that $Df[P_N(\theta)]^{-1}$ is an $\bar{N}$-th order polynomial with matrix coefficients. Then we let

$$Df[P_N(\theta)]^{-1} = \sum_{0\leq|\alpha|\leq\bar{M}} C_\alpha \theta^\alpha$$

where the coefficients C_α, depend on the B_β and c_α, can be worked out via Cauchy Products.

Let $Q_0 \Sigma Q_0^{-1} = Df(p)$ be the eigenvector/eigenvalue decomposition of the differential and note that

$$C_0 = Df[P_N(0)]^{-1} = Df(p)^{-1} = Q_0^{-1}\Sigma^{-1}Q_0.$$

Then

$$\begin{aligned}\|Df[P_N]^{-1}\|_{\Sigma,\nu} &\leq \left\| Q_0^{-1}\Sigma^{-1}Q_0 + \sum_{1\leq|\alpha|\bar{M}} C_\alpha\theta^\alpha \right\|_{\Sigma,\nu} \\ &\leq \|Q_0\|\|Q_0^{-1}\|\mu_*^{-1} + \sum_{|\alpha|=1}^{\bar{N}} \|C_\alpha\|\nu^{|\alpha|}.\end{aligned}$$

Then we define C_1 and C_2 to be any bounds of the form

$$\|Q_0\|\|Q_0^{-1}\| \leq C_1,$$

and

$$\sum_{|\alpha|=1}^{\bar{N}} \|C_\alpha\|\nu^{|\alpha|} \leq C_2.$$

Note that since these expressions involve bounding finite sums of known quantities, both C_1 and C_2 are easily found using interval arethmetic. Finally we have that

$$\|Df[P_N]\|_{\Sigma,\nu} \leq C_1 \mu_*^{-1} + C_2. \tag{4.19}$$

as needed in the definition of the validation values.

Of course if f is not a polynomial map it is possible to make a similar argument using at M-th order Taylor expansion by including a remainder term. This is a technicality not needed in the present work but which could be easily added to the scheme. In this case C_2 would simply have to incorporate as well the truncation error on the ball of radius ρ'.

5. Rigorous Computation of Transverse Homoclinic Orbits. Throughout this section we make the following definitions and assumptions.

- P1: Let $p \in \mathbb{R}^n$ be a hyperbolic fixed point of the analyticomorphism $f : \mathbb{R}^n \to \mathbb{R}^n$. Assume that $Df(p)$ is diagonalizable, and that n_s, $n_u > 0$, the number of stable and unstable eigenvalues respectively, have $n_u + n_s = n$.
- P2: Let P_N be the N-th order polynomial approximate parameterization of $W^u(p)$. In addition let ν_u, ϵ_u, C_1^u, C_2^u, ρ, ρ', and μ_*, μ^* be validation values for P_N. Assume that these validation values satisfy the hypotheses of Theorem (4.1) applied to f^{-1}, so that the is a unique analytic N-tail h with $\|h\|_{\nu_u} \leq \delta_u$ so that $P = P_N + h$ is a parameterization of $W^u_{\text{loc}}(p)$.
- P3: Similarly, let Q_N be the N-th order polynomial approximate parameterization of $W^s(p)$ and ν_s, ϵ_s, C_1^s, C_2^s, ρ, ρ', and μ_-, μ^+ be validation values for Q_N and assume that these validation values satisfy the hypotheses of Theorem 4.1 so that the is a unique analytic N-tail g with $\|g\|_{\nu_u} \leq \delta_s$ so that $Q = Q_N + g$ is a parameterization of $W^s_{\text{loc}}(p)$.

Then we can write the homoclinic functional equation (Equation 1.3) in the form

$$F(\theta, x_1, x_2, \ldots, x_{k-2}, x_{k-1}, \phi) =$$

$$\begin{bmatrix} f^{-1}(x_1) - P_N(\theta) - h(\theta) \\ f^{-1}(x_2) - x_1 \\ f^{-1}(x_3) - x_2 \\ \vdots \\ f^{-1}(x_j) - x_{j-1} \\ f(x_j) - x_{j+1} \\ \vdots \\ f(x_{k-2}) - x_{k-1} \\ f(x_{k-1}) - Q_N(\phi) - g(\phi) \end{bmatrix} \equiv F_N(\theta, x_1, \ldots, x_{k-1}, \phi) + H(\theta, \phi), \tag{5.1}$$

where again we stress that P_N and Q_N are explicitly know polynomials and h, and g are unknown analytic N-tails for which we have the mathematically rigorous bounds given in $P3$. We call F_N the *discretized homoclinic functional equation.*

Heuristically our validation scheme is as follows. Assume that there is $\hat{x} = (\hat{\theta}, \hat{x}_1, \ldots, \hat{x}_{k-1}, \hat{\phi}) \in \mathbb{R}^{nk}$ with $\hat{\theta} \in B_u^\circ$ and $\hat{\phi} \in B_s^\circ$ having that $\hat{x}$ is an approximate zero of the discretized homoclinic equation, i.e. assume that

$$\|F_N(\hat{x})\| \approx 0.$$

If in addition δ_s and δ_u are small, then we have that $\hat{x}$ is also an approximate zero of F, so that $\text{orbit}(\hat{x}_j)$ is approximately homoclinic to p for each $1 \leq j \leq k-1$. Our goal is to apply the Newton-Kantorovich Theorem (Thm 4.3) in order to conclude that there exists a true solution x_* of the full homoclinic functional equation near $\hat{x}$. These notions are formalized in the next section.

5.1. Validation of Homoclinic Connections. We now formalize the heuristic scheme just described. Assume, in addition to $P1$, $P2$ and $P3$, that we have computed, or are otherwise given, the following "quasi-local" data, which we refer to as *homoclinic validation values.*

Definition 5.1 (Homoclinic validation values). We say that the vector $\hat{x} = (\hat{\theta}, \hat{x}_1, \ldots, \hat{x}_{k-1}, \hat{\phi}) \in \mathbb{R}^{nk}$, and positive constants A_N, M_N, C_β, C_P, κ, $\hat{\delta}$, $\hat{\epsilon}$, and r are *validation values* for the homoclinic functional equation if the following conditions are met:

1. Define the point $x_0 \in \mathbb{R}^{nk}$ to be given by $x_0 = (0_{n_u}, p, \ldots, p, 0_{n_s})$ where p is the fixed point of f described in $P1 - P3$ and 0_{n_u} and 0_{n_s} are the zero vectors in $\mathbb{R}^{n_u}$ and $\mathbb{R}^{n_s}$. Assume that x_0 is not in the poly-disk $B_r(\hat{x}) \subset \mathbb{R}^{nk}$.
2. $\hat{x} = (\hat{\theta}, \hat{x}_1, \ldots, \hat{x}_{k-1}, \hat{\phi}) \in \mathbb{R}^{nk}$ is an $\hat{\epsilon}$-approximate solution of $F = 0$, in the sense that
$$|DF_N(\hat{x})^{-1} F_N(\hat{x})| \leq \hat{\epsilon}.$$
3. $DF_N(\hat{x})$ is non-singular and the positive constant A_M has that $\|DF_N(\hat{x})^{-1}\|_M \leq A_N$.
4. $|\hat{\theta}| < \nu_u$ and $|\hat{\phi}| < \nu_s$ so that we can define what we will call *the first order loss of domain parameters*
$$\hat{\sigma}_s = -\ln\left(\frac{|\hat{\theta}|}{\nu_s}\right), \qquad \textit{and} \qquad \hat{\sigma}_u = -\ln\left(\frac{|\hat{\phi}|}{\nu_u}\right).$$
5. The positive constant M_N has that
$$\left(\max_{1\leq i\leq nk} \sum_{j=1}^{n} [DF_N^{-1}(\hat{x})]_{ij}\right) \frac{2\pi n_u}{\nu_u \hat{\sigma}_u} \delta_u + \left(\max_{1\leq i\leq nk} \sum_{j=nk-n+1}^{nk} [DF_N^{-1}(\hat{x})]_{ij}\right) \frac{2\pi n_s}{\nu_s \hat{\sigma}_s} \delta_s \leq M_N.$$
6. The positive constant $\hat{\delta}$ has that
$$\left(\max_{1\leq i\leq nk} \sum_{j=1}^{n} [DF_N^{-1}(\hat{x})]_{ij}\right) \delta_u + \left(\max_{1\leq i\leq nk} \sum_{j=nk-n+1}^{nk} [DF_N^{-1}(\hat{x})]_{ij}\right) \delta_s. \leq \hat{\delta}.$$
7. The parameters $\hat{\theta}$, $\hat{\phi}$ and the positive constant r also satisfy $|\hat{\theta}| + r < \nu_u$ and $|\hat{\phi}| + r < \nu_s$ so that we can define the *second order loss of domain parameters*
$$\sigma_s = -\ln\left(\frac{|\hat{\theta}| + r}{\nu_s}\right), \qquad \textit{and} \qquad \sigma_u = -\ln\left(\frac{|\hat{\phi}| + r}{\nu_u}\right).$$
8. The positive constant C_β has that
$$\max_{1\leq j\leq k-1} \max_{1\leq i\leq n} \max_{|\beta|=2} \left\{ \|\partial^\beta f_i\|_{B_r(\hat{x}_j)}, \|\partial^\beta f_i^{-1}\|_{B_r(\hat{x}_j)} \right\} \leq C_\beta.$$
9. The positive constant C_P has
$$\max\left(\|D^2 P_N\|_{B_r(\hat{\theta})} + \frac{2\pi^2 n^2}{\nu_u^2 \sigma_u^2} \delta_u, \;\; \|D^2 Q_N\|_{B_r(\hat{\phi})} + \frac{2\pi^2 n^2}{\nu_s^2 \sigma_s^2} \delta_s \right) \leq C_P.$$
10. Finally, κ is positive constant having
$$N_f C_\beta + C_P \leq \kappa,$$
where N_f is the max of the number of non-zero second partials of f and f^{-1}.

We sometimes write $C_\beta(r)$, $C_P(r)$ and $\kappa(r)$ to emphasize that these constants should be thought of as depending on the radius r of the $\mathbb{R}^{nk}$ poly-disk about $\hat{x}$. In other words they are the members of a validation values set which carry global information about the ball $B_r(\hat{x}) \subset \mathbb{R}^{nk}$. In the next section we will prove the following *a-posteriori* result for F, which is based on a standard Newton-Kantorivich argument combined with the rigorous a-posteriori bounds on the parameterizations.

THEOREM 5.1 (A-posteriori validation of a homoclinic connection). *Given assumptions* $[P1]-[P3]$ *let* $\hat{x}$, A_N, M_N, C_{beta}, C_P, κ, $\hat{\delta}$, $\hat{\epsilon}$, *and* r *be a set of homoclinic validation values as in Def 5.1. We call* ϵ_{NK} *a "Newton-Kantorovich Epsilon" if*

$$\frac{1}{1-M_N}\left(\hat{\epsilon}+\hat{\delta}\right) \leq \epsilon_{NK}. \tag{5.2}$$

With ϵ_{NK} *fixed suppose that*

A. $0 < M_N < 1$,

B. $2\epsilon_{NK} \leq r$,

C. $\frac{A_N}{1-M_N} 4\kappa\epsilon_{NK} \ \leq \ 1$.

Then there is a unique $x_* \in B_r(\hat{x}) \subset \mathbb{R}^{nk}$ *which is a non-trivial solution of the equation* $F(x_*) = 0$. *Such an* x_* *clearly has that*

$$|x_* - \hat{x}| \leq r.$$

Moreover, if for all $x \in B_r(\hat{x}) \subset \mathbb{R}^{nk}$ *we have both that* $DF_N(x)^{-1}$ *exists, and that*

$$\|DF_N(x)^{-1}DH(x)\|_{M,B_r(\hat{x})} < 1, \tag{5.3}$$

then it follows that $W^s(p) \cap W^u(p)$, *which is non-empty due to the existence of* x_*, *is also transverse.*

5.2. Proof of Theorem 5.1. The proof consists of two parts. First we use Theorem 4.3 to show that the hypotheses of Theorem 5.1 combined with the definition of homoclinic validation values imply the existence of a non-trivial zero of F in $B_r(\hat{x})$. Then we study the form of the differential in order to establish the transversality. The subtly throughout is that while $F_N(\hat{x})$ and $DF_N^{-1}(\hat{x})$ are known, it is F and DF which must be explicitly bound.

In order to apply the Newton-Kantorovic Theorem (thm 4.3) we must show that

(i) $DF(\hat{x})$ has bounded inverse,

(ii) DF is Lipschitz on $B_r(\hat{x})$ with Lipschitz constant κ,

(I) $|DF(\hat{x})^{-1}F(\hat{x})| \leq \varepsilon_{NK}$,

(II) $\varepsilon_{NK} \leq r/2$,

(III) $4\varepsilon_{NK}\kappa\|DF(\hat{x})^{-1}\|_M \leq 1$.

Here the roman numerals refer to the nomenclature established in the statement of Theorem 4.3.

Let $[DF_N^{-1}(\hat{x})]_{(a:b)}$, with $a < b \in \mathbb{N}$, denote the submatrix of $DF_N^{-1}(\hat{x})$ composed of columns a through b. We begin by noting that

$$\begin{aligned} DF_N^{-1}(\hat{x})DH(\hat{x}) &= DF_N^{-1}(\hat{x})\begin{bmatrix} D_\theta h(\hat{\theta}) & 0 & \dots & 0 \\ 0 & 0 & \dots & 0 \\ \vdots & \vdots & \dots & \vdots \\ 0 & 0 & \dots & D_\phi g(\hat{\phi}) \end{bmatrix} \\ &= \left[[DF_N^{-1}(\hat{x})]_{(1:n)}Dh(\hat{\theta}) \mid 0 \mid \ \dots \ \mid 0 \mid [DF_N^{-1}(\hat{x})]_{(nk-n+1:nk)}Dg(\hat{\phi})\right], \end{aligned}$$

so that

$$
\begin{aligned}
\|DF_N^{-1}(\hat{x})DH(\hat{x})\|_M &\leq \left(n_u \max_{1\leq i\leq nk} \sum_{j=1}^{n} [DF_N^{-1}(\hat{x})]_{ij}\right) \|Dh\|_{\nu_u e^{-\hat{\sigma}_u}} \\
&+ \left(n_s \max_{1\leq i\leq nk} \sum_{j=nk-n+1}^{nk} [DF_N^{-1}(\hat{x})]_{ij}\right) \|Dg\|_{\nu_s e^{-\hat{\sigma}_s}} \\
&\leq M_N \\
&< 1,
\end{aligned}
$$

by part 5 of Definition 5.1, The Cauchy bounds of Lemma (4.3), and Assumption A of the present Theorem. It follows from the Neumann Series Theorem that the matrix $I + DF_N^{-1}(\hat{x})DH(\hat{x})$ is invertible and that

$$
\left\| [I + DF_N^{-1}(\hat{x})DH(\hat{x})]^{-1} \right\|_M \leq \frac{1}{1 - M_N}. \tag{5.4}
$$

Then we have that

$$
\begin{aligned}
DF(\hat{x})^{-1} &= [DF_N(\hat{x}) + DH(\hat{x})]^{-1} \\
&= \left[DF_N(\hat{x})\ \left(I + DF_N(\hat{x})^{-1}DH(\hat{x})\right)\ \right]^{-1} \\
&= [I + DF_N(\hat{x})^{-1}DH(\hat{x})]^{-1}\ DF_N(\hat{x})^{-1}
\end{aligned} \tag{5.5}
$$

exists, and obtain the bound

$$
\|DF(\hat{x})^{-1}\|_M \leq \frac{A_N}{1 - M_N}. \tag{5.6}
$$

This establishes (i) of Theorem 4.3.

In order to investigate the Lipschitz condition on the differential DF we define the real valued functions $g_{ij} : B_r(\hat{x}) \subset \mathbb{R}^{nk} \to \mathbb{R}$ where $1 \leq i, j \leq nk$ by the expressions

$$
g_{ij}(z) = \partial_j F_i(z).
$$

Then for $x, y \in B_r(\hat{x})$ we have that

$$
\begin{aligned}
|g_{ij}(x) - g_{ij}(y)| &\leq \|\nabla g_{ij}\|_{M, B_r(\hat{x})} |x - y| \\
&\leq \sum_{\ell=1}^{nk} \|\partial_\ell g_{ij}\|_{B_r(\hat{x})} |x - y| \\
&\leq \left(\sum_{\ell=1}^{nk} \|\partial_\ell \partial_j F_i\|_{B_r(\hat{x})}\right) |x - y|,
\end{aligned} \tag{5.7}
$$

by the Mean Value Theorem. Then

$$
\begin{aligned}
\|DF(x)-DF(y)\|_M \equiv & \sup_{\substack{v\in\mathbb{R}^{nk}\\ |v|=1}} |[DF(x)-DF(y)]v| \\
\leq & \max_{1\leq i\leq nk} \sum_{1\leq j\leq nk} |[DF(x)-DF(y)]_{ij}| \\
= & \max_{1\leq i\leq nk} \sum_{1\leq j\leq nk} |\partial_j F_i(x)-\partial_j F_i(y)| \\
\leq & \left(\max_{1\leq i\leq nk} \sum_{j=1}^{nk}\sum_{\ell=1}^{nk} \|\partial_\ell\partial_j F_i\|_{B_r(\hat{x})}\right)|x-y|, \qquad (5.8)
\end{aligned}
$$

where we have used the estimate of Inequality 5.7.

Note that from 7 of Definition 5.1 and the Cauchy Bounds of Lemma 4.3 we have that for any $1\leq i\leq n$

$$
\begin{aligned}
\|\partial_\ell\partial_j h_i\|_{B_r(\hat{x})} &= \|\partial_\ell\partial_j h_i\|_{B_r(\hat{\theta})} \\
&\leq \|\partial_\ell\partial_j h_i\|_{\nu_u e^{-\sigma_u}} \\
&\leq \frac{2\pi^2}{\nu_u^2\sigma_u^2}\delta_u,
\end{aligned}
$$

and similarly

$$
\|\partial_\ell\partial_j g_i\|_{B_r(\hat{x})} \leq \frac{2\pi^2}{\nu_s^2\sigma_s^2}\delta_s.
$$

Using these estimates and considering the second partial derivatives of F one component at a time we recall 8, 9, and 10 of Definition 5.1 and obtain that

$$
\max_{1\leq i\leq nk}\sum_{j=1}^{nk}\sum_{\ell=1}^{nk}\|\partial_\ell\partial_j F_i\|_{B_r(\hat{x})} \leq N_f C_\beta + C_P = \kappa.
$$

Combining this with Inequality (5.8) gives (ii) of Theorem 4.3.

For (I) of Theorem 4.3 we use the notation $[DF_N^{-1}(\hat{x})]_{(a:b)}$ as above and have that

$$
\begin{aligned}
\left|DF_N^{-1}(\hat{x})H(\hat{x})\right| &= \left| DF_N^{-1}(\hat{x}) \begin{bmatrix} h(\hat{\theta}) \\ 0 \\ \vdots \\ 0 \\ g(\hat{\phi}) \end{bmatrix} \right| \\
&= \left| [DF_N^{-1}(\hat{x})]_{(1:n)}\ h(\hat{\theta}) + [DF_N^{-1}(\hat{x})]_{(nk-n+1:nk)}\ g(\hat{\phi}) \right| \\
&\leq \left(\max_{1\leq i\leq nk}\sum_{j=1}^{n}\left|[DF_N^{-1}(\hat{x})]_{ij}\right|\right)\|h\|_{\nu_u} \\
&+ \left(\max_{1\leq i\leq nk}\sum_{j=nk-n+1}^{nk}\left|[DF_N^{-1}(\hat{x})]_{ij}\right|\right)\|g\|_{\nu_s} \\
&\leq \hat{\delta}, \qquad (5.9)
\end{aligned}
$$

where we have used 6 of Definition 5.1. Then, recalling Equation 5.5 and Inequality 5.6 we have

$$
\begin{aligned}
\left|DF(\hat{x})^{-1}F(\hat{x})\right| &\leq \left|[I + DF_N(\hat{x})^{-1}DH(\hat{x})]^{-1}\ DF_N(\hat{x})^{-1}F(\hat{x})\right| \\
&= \left|[I + DF_N(\hat{x})^{-1}DH(\hat{x})]^{-1}\ DF_N(\hat{x})^{-1}\left(F_N(\hat{x}) + H(\hat{x})\right)\right| \\
&\leq \frac{1}{1-M_N}\left(\left|DF_N^{-1}(\hat{x})F_N(\hat{x})\right| + \left|DF_N^{-1}(\hat{x})H(\hat{x})\right|\right) \\
&\leq \frac{1}{1-M_N}\left(\hat{\epsilon} + \hat{\delta}\right) \\
&\leq \epsilon_{NK},
\end{aligned} \tag{5.10}
$$

where we have used 2 of Definition 5.1, the Estimate given by Inequality 5.9, and the the defintion of ϵ_{NK} given by Equation 5.2. This establishes condition (I) of Theorem 4.3. Finally note that (III) of Theorem 4.3 follows directly from assumption C of the present theorem and Inequality 5.6, while (II) of Theorem 4.3 is assumption B of the present Theorem.

Then the conditions of Theorem 4.3 are satisfied and we obtain the existence of a unique $x_* \in B_r(\hat{x})$ so that $F(x_*) = 0$. Note that since $x_* \neq x_0$ by 1 of Definition 5.1, we obtain a non-trivial homoclinic orbit.

Now we turn to the question of transversality of the intersection at x_*. An argument similar to the one used to derive Equation 5.5, except with $\hat{x}$ replaced by a variable $x \in B_r(\hat{x})$ shows that $DF(x)$ is invertible for all $x \in B_r(\hat{x})$ as long as $DF_N(x)$ is invertible for all $x \in B_r(\hat{x})$ and the condition given by Equation 5.3 is met. Since we have assumed that both of these conditions are met, it follows that $DF(x_*)$ is non-singular.

What remains is to show is that the non-singularity of $DF(x_*)$ implies that the homoclinic orbit is transverse. Assume for the moment that $k = 1$, so that the local manifolds $W^u_{\text{loc}}(p) = P[B_{\nu_u}(0)]$ and $W^s_{\text{loc}}(p) = Q[B_{\nu_s}(0)]$ intersect at x_*. In this case the operator F reduces to

$$
F(\theta, \phi) = P(\theta) - Q(\phi).
$$

and we have a solution $x_* = (\theta_*, \phi_*) \in B_r(\hat{x})$. Since $DF(x_*)$ is non-singular, the columns of

$$
DF(x_*) = [D_\theta P(\theta_*)| - D_\phi Q(\phi_*)]
$$

span $\mathbb{R}^n$. But the columns of $D_\theta P(\theta_*)$ and $D_\phi Q_{\phi_*}$ span $T_{P(\theta_*)}W^u(p)$ and $T_{Q(\phi_*)}W^s(p)$ respectively. It follows that $T_{P(\theta_*)}W^u(p)$ and $T_{Q(\phi_*)}W^s(p)$ span $\mathbb{R}^n$, which is to say that x_* is a point of transverse intersection.

Now suppose $K > 1$, and $x_* \in \mathbb{R}^{nk}$ is the solution of $F = 0$. Since any f-iterate of a local unstable manifold is again a local unstable manifold, and any f-iterate of a homoclinic point is another homoclinic point, we have that the local unstable manifold $f^k[W^u_{\text{loc}}(p)] = f^k[P(B_{n_u}(0))]$ intersects $W^s_{\text{loc}}(p) = Q[B_{\nu_s}(0)]$ at the phase space point $Q(\phi_*) = f^k[P(\theta_*)]$. Then we are in exactly the same situation as above, and the intersection is transverse if and only if the matrix

$$
[-D_\theta f^k[P(\theta_*)]\,|D_\phi Q(\phi_*)] = [-D_x f^k[P(\theta_*)]D_\theta P(\theta_*)|D_\phi Q(\phi_*)]
$$

is non-singular. Note that $D_x f^k(x)$ is non-singular for any $x \in \mathbb{R}^n$ as f is a diffeomorphism.

Now, by hypothesis the matrix

$$
DF(x_*) = \begin{pmatrix} -D_\theta P(\theta_*) & & 0 \\ \vdots & \mathbf{A} & \vdots \\ 0 & & -D_\phi Q(\phi_*) \end{pmatrix},
$$

is non-singular, so that if we construct the non-singular matrix

$$\mathbf{B} = \begin{pmatrix} D_x f^k[P(\theta_*)] & \mathbf{0} \\ \mathbf{0} & Id_{n(k-1)\times n(k-1)} \end{pmatrix}$$

and multiply, we have that the product

$$\mathbf{B}DF(x_*) = \begin{pmatrix} -D_x f^k[P(\theta_*)]D_\theta P(\theta_*) & & 0 \\ \vdots & \mathbf{C} & \vdots \\ 0 & & -D_\phi Q(\phi_*) \end{pmatrix}$$

is the product of non-singular matrices hence is itself non-singular (here the actual form of $\mathbf{C}$ is unimportant to us). Since $\mathbf{B}DF(x_*)$ is non-singular, it has linearly independent columns. Exploiting this linear independence gives that the columns of

$$[-D_\theta f^k[P(\theta_*)]\,|D_\phi Q(\phi_*)] = [-D_x f^k[P(\theta_*)]D_\theta P(\theta_*)|D_\phi Q(\phi_*)],$$

span $\mathbb{R}^n$, which is to say that the local manifolds $W^s_{\text{loc}}(p) = Q[B_{\nu_s}(0)]$ and $W^u_{\text{loc}}(p) = f^k[P(B_{\nu_u}(0)]$ intersect transversally, as desired.

□

6. Computer Assisted Proofs of Transverse Homoclinic Orbits and Chaos. We begin by considering a Lomelí Map with parameters $a = 0.5$, $b = -0.5$, $c = 1$, $\alpha = -5.34$, and $\tau = 0.8$. These correspond to Dullin-Meiss parameters of $\bar{a} = 1$, $\bar{b} = 0.5$, $\bar{c} = 0.5$, $\mu = -2.4$ and $\epsilon = 5.5$. For these parameters values there is a hyperbolic fixed point at $p = (x_-, x_-, x_-)$ with $x_- = -2.745207879911715$. Then $Df(p)$ has unstable complex conjugate eigenvalues $-0.402451645443971 \pm i2.035392592347574$ and stable eigenvalue 0.232299350932085. Table 6 illustrates the results of the parameterization computations, which are carried out using the rigorous interval arithmetic library IntLab (which runs under Matlab).

The table records the dimension of the manifolds, the approximation order N used in each case, the time taken to compute the coefficients of the polynomial approximations P_N and Q_N, the time taken to a-posteriori validated the approximations, the magnitudes of the resulting bounds on the truncation errors $\|h\|_{\nu_u} = \delta_u$ and $\|g\|_{\nu_s} = \delta_s$, the size of the parameter domain radii ν_u and ν_s, the size of the eigenvector scaling, and finally a rigorous bound on the size of the local manifolds in the sigma-norm.

Dim	Order	Approx Time	Valid Time	Validated Error	Radius	$\lvert\xi\rvert$	$\lVert\cdot\rVert_{\nu,\Sigma}$
1	50	5.16 sec	0.40 sec	8.71×10^{-13}	0.9	2	1.96
2	25	1.68 min	2.84 sec	5.67×10^{-12}	0.4	1.5	1.21

TABLE 6.1
Manifold Validation Performance: Example 1 ($\epsilon = 5.5, \mu = -2.4$)

We then use a classical, numerical Newton scheme to find an approximate numerical solution to the discretized homoclinic functional equaiton $F_N(x) = 0$ with $k = 6$ and of course $n = 3$. This leads to an approximate zero

$$\hat{x} = \begin{bmatrix} \hat{\theta} \\ \hat{x}_1 \\ \hat{x}_2 \\ \hat{x}_3 \\ \hat{x}_4 \\ \hat{x}_5 \\ \phi \end{bmatrix} = \begin{bmatrix} (-0.337379322019076, 0.088431234641040) \\ (-1.648314148155201, -3.605864990373435, -2.750773367689280) \\ (1.979508268106647, -1.648314148155201, -3.605864990373435) \\ (-1.054666610773029, 1.979508268106647, -1.648314148155201) \\ (-2.313572985270695, -1.054666610773029, 1.979508268106647) \\ (-2.642742570718999, -2.313572985270695, -1.054666610773029) \\ 0.228218016117584 \end{bmatrix}$$

K	$\hat{x}_1$	r
6	$(-1.648314148155201, -3.605864990373435, -2.750773367689280)$	1.1×10^{-11}
6	$(-1.692334813290302, -3.652591337627915, -2.718741184627647)$	1.06×10^{-11}

TABLE 6.2

Primary Intersection Validation ($\epsilon = 5.5, \mu = -2.4$): 3.21 sec for proof of both orbits. Chaos confirmed in both cases.

Using Theorem 5.1 we can validate that there is a true solution of the homoclinic functional equation in a polydisk $B_r(\hat{x})$ with $r = 1.1 \times 10^{-11}$. Table 6 gives computation data for the proof just described, and also for the proof of a second distinct solution of the homoclinic operator equation for $k = 6$. In each case only the $\hat{x}_1$ data is recorded. Figure 6.1 shows the time series data for the x component of the first of these two orbits. Black dots represent points in $\hat{x}$. Red points represent iterates on the local manifolds.

We note that in these first two proofs is that the time taken to compute the rigorous interval enclosures of the coefficients for the two variable polynomial P_N is 1 minute 68 seconds, while the validation of the two homoclinic orbits takes only 3.21 seconds. Since we can use the same polynomial approximations P_N and Q_N in any homoclinic functional equation, regardless of the size of k, we compute 32 more distinct homoclinic orbits with k varying. The results are tabulated in Table 6, and again only $\hat{x}_1$ components are recorded. Note that the time required to validate all 34 of orbits is a little less than the time needed to compute the rigorous approximation of the stable manifold. This suggests that high order approximation of the manifolds is most useful when computing many distinct homoclinic orbits at a given parameter set. Figures 6.2 and 6.3 show time series data for the x-component of the shortest and longest homoclinic orbits validated.

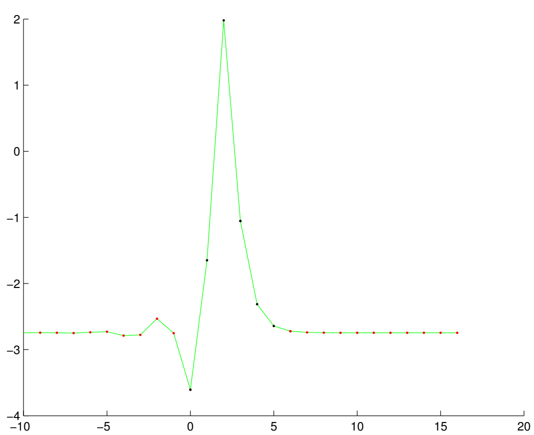

FIG. 6.1. *x-axis projection of the validated homoclinic; $k = 6$, $\epsilon = 5.5$.*

We note that in the previous example the dynamics is “fast” in the sense that as few as 6 iterates are needed in order to transition from the local unstable to the local stable manifold. In order to compute orbits with longer ‘time of flight’ (higher k) we consider a Lomelí map with parameters a, b, c, and τ as before, but with $\alpha = -0.04$. This corresponds to a Dullin-Meiss value of $\epsilon = 0.2$ with all other parameters as above. At these parameter values we study the fixed point $p = (x_-, x_-, x_-)$ with $x_- = -0.847213595499957$. The differential $Df(p)$ has unstable complex conjugate eigenvalues of $-0.150742620101308 \pm i1.205183554810613$ and a stable eigenvalue of 0.677878442452638. The data for the parameterization computations

K	$\hat{x}_1$	r	time
8	$(-1.878269557294666 - 3.704360821688669 - 2.644177124855255)$	1.0×10^{-11}	3.13 sec
$\cdot$	$(-1.598486534326447 - 3.712394711133192 - 2.715338895232408)$	1.1×10^{-11}	$\cdot$
9	$(-1.693365888596068 - 3.516449414154529 - 2.776271298390562)$	1.05×10^{-11}	4.95 sec
$\cdot$	$(-2.033965491062911 - 3.691036738831221 - 2.607784382423848)$	1.05×10^{-11}	$\cdot$
$\cdot$	$(-3.649752275192224 - 2.876479215542708 - 2.487231377447373)$	1.00×10^{-11}	$\cdot$
11	$(-1.724921906236488 - 3.503098391735548 - 2.773685700840596)$	1.06×10^{-11}	10.1 sec
$\cdot$	$(-2.089900084565888 - 3.686144425839955 - 2.594568562106802)$	1.0×10^{-11}	$\cdot$
$\cdot$	$(-3.634873256589227 - 2.906134859387798 - 2.482573305537549)$	1.0×10^{-11}	$\cdot$
$\cdot$	$(-3.620917995724487 - 2.915222901577827 - 2.483676082433866)$	1×10^{-11}	$\cdot$
$\cdot$	$(-2.114585182128023 - 3.679401143907701 - 2.591096188024756)$	1.03×10^{-11}	$\cdot$
$\cdot$	$(-1.768297176557754 - 3.496683655844906 - 2.765421447288818)$	1.05×10^{-11}	$\cdot$
12	$(-1.613946132963925 - 3.601054205346514 - 2.761528716808955)$	1.1×10^{-11}	6.8 sec
$\cdot$	$(-1.672093712060165 - 3.527103879468739 - 2.777334962197874)$	1.06×10^{-11}	$\cdot$
$\cdot$	$(-2.122097145983667 - 3.674130503709248 - 2.591708802528494)$	1.04×10^{-11}	$\cdot$
$\cdot$	$(-1.822510500455057 - 3.571768208555173 - 2.720873332899369)$	1.1×10^{-11}	$\cdot$
13	$(-3.644121861531430 - 2.872709464400592 - 2.489856336907984)$	1×10^{-11}	10.35 sec
$\cdot$	$(-1.720320939862523 - 3.656391590596805 - 2.709687450800172)$	1.0×10^{-11}	$\cdot$
$\cdot$	$(-1.972320520664557 - 3.693712699582179 - 2.623618282117915)$	1.0×10^{-11}	$\cdot$
$\cdot$	$(-3.647170226591191 - 2.867372482172479 - 2.490553201321108)$	1×10^{-11}	$\cdot$
$\cdot$	$(-1.582489566947040 - 3.527839146851471 - 2.799122415227350)$	1.07×10^{-11}	$\cdot$
$\cdot$	$(-1.574224069064366 - 3.529792848481951 - 2.800384605320380)$	1.1×10^{-11}	$\cdot$
20	$(-1.931148725862011 - 3.707646666557216 - 2.627909579872393)$	1.0×10^{-11}	4.01 sec
$\cdot$	$(-3.638326627639060 - 2.901176380906034 - 2.483107270172258)$	1.0×10^{-11}	
21	$(-3.690719490424216 - 2.823690393936636 - 2.490880594199791)$	1×10^{-11}	16.44 sec
$\cdot$	$(-1.957194765763665 - 3.705297800511473 - 2.621878341459779)$	1.05×10^{-11}	$\cdot$
$\cdot$	$(-1.729640666364290 - 3.510087223951199 - 2.769773329564600)$	1.06×10^{-11}	$\cdot$
$\cdot$	$(-1.690639165363386 - 3.669844178437995 - 2.711227287037635)$	1.1×10^{-11}	$\cdot$
$\cdot$	$(-1.950380561442004 - 3.705777860019821 - 2.623527619587280)$	1.1×10^{-11}	$\cdot$
$\cdot$	$(-3.702924845715120 - 2.791265552326865 - 2.496202529149488)$	1.0×10^{-11}	$\cdot$
$\cdot$	$(-3.708117158393551 - 2.774277602263187 - 2.499173703371658)$	0.98×10^{-11}	$\cdot$
$\cdot$	$(-1.932029291989042 - 3.707691973193318 - 2.627641932935536)$	1.04×10^{-11}	$\cdot$
$\cdot$	$(-3.616786394029812 - 2.918973341522530 - 2.483676503055390)$	1×10^{-11}	$\cdot$

Table 6.3

Secondary Homoclinic Orbits ($\epsilon = 5.5, \mu = -2.4$): Total Time for Proofs: 55.0 sec. Transversality confirmed in all cases.

Dim	Order	Approx Time	Proof Time	Validated Error	Radius	$\lvert\xi\rvert$	$\lVert \cdot \rVert_\nu$
1	50	4.95 sec	0.45 sec	2.71×10^{-11}	0.9	1.5	5.63
2	25	1.66 min	2.94 sec	4.30×10^{-13}	0.4	0.5	0.32

Table 6.4

Manifold Validation Performance: Example 2 ($\epsilon = 0.2, \mu = -2.4$)

is given in Table 6, with format identical to before. Table 6 gives data for the results of the homoclinic validation computations for five different orbits with values of k varying between 75 and 121. Figures 6.3 and 6.4 show time series data for the shortest and longest of these homoclinic orbits (x-component in both cases). Note that for the orbit with $k = 121$ the discretized homoclinic functional equation $F_N : \mathbb{R}^{nk} \to \mathbb{R}^{nk}$ has $nk = 121 \times 3 = 363$.

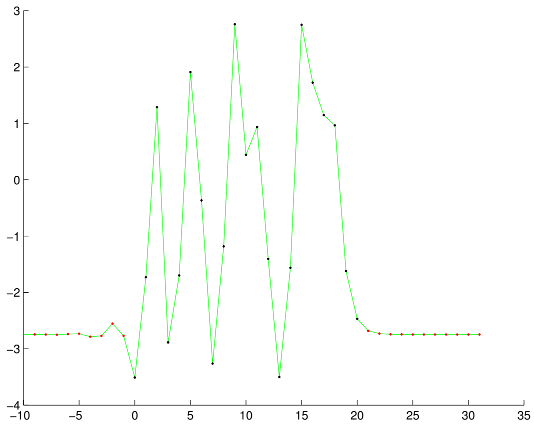

FIG. 6.2. *x-axis projection of the validated homoclinic; $k = 21$, $\epsilon = 5.5$.*

K	$\hat{x}_1$	r	time
75	$(-0.7172485197141 97 - 1.043252947479510 - 0.860812112677259)$	1.04×10^{-7}	6.32 sec
76	$(-1.107394504655081 - 0.745731963636135 - 0.642025567084575)$	1.4×10^{-7}	6.15 sec
111	$(-1.104148108665029 - 0.729631044649217 - 0.648872760710501)$	1.05×10^{-7}	15.04 sec
118	$(-1.087535686140795 - 0.715568561563514 - 0.669111490970251)$	1.3×10^{-7}	16.11 sec
121	$(-0.995810895350469 - 0.972045779061998 - 0.671276957464922)$	1.04×10^{-7}	18.6 sec

TABLE 6.5
Homoclinic Orbits ($\epsilon = 0.2, \mu = -2.4$): Transversality confirmed in all cases.

Finally we cary out a similar computation for the map $G : \mathbb{R}^6 \to \mathbb{R}^6$ obtained by a coupling a pair of Lomelí maps as discussed in Section 2.1. We take parameters $a_1 = a_2 = 0.5$, $b_1 = b_2 = -0.5$, $c_1 = c_2 = 1$, $\tau_1 = \tau_2 = 0.8$, $\alpha_1 = -5.339999999999998$ and $\alpha_2 = -5.939999999999998$ (corresponding to Dullin-Meiss parameters of $\epsilon_1 = 5.5$ and $\epsilon_2 = 6.1$). The maps are coupled with a strength of $\varepsilon = 5 \times 10^{-7}$. The reason for the small coupling strength is that we obtain a numerical guess by continuing away from the product system having $\varepsilon = 0$. The coupled system is quite sensitive to this parameter, and a tangency develops for coupling strengths much larger than this. However our proof does not in any way depend on the use of the small parameter, other than that it is helpful for locating an initial guess for a homoclinic in coupled system. We have made no attempt at an exhaustive study of the six dimensional system. The coupled system only serves to illustrate that the computations go through in higher dimensions.

We study the fixed point $p = (x_-^1, x_-^1, x_-^1, x_-^2, x_-^2, x_-^2)$ with $x_-^1 = -2.74507879911714$ and $x_-^2 = -2.869817807045693$. The differential $DG(p)$ has two pair of unstable complex conjugate eigenvalues $-0.428678184042694 \pm i2.076458156435394$ and $-0.402451645448668 \pm i2.035392592342751$, and a pair of real distinct stable eigenvalues 0.232299350933555 and 0.222447464570467. Then fixed point has a four dimensional unstable manifold and a two dimensional stable manifold. We show that these manifolds intersect transversally using the arguments developed above. The results of the computer assisted proofs are recorded in Tables 6.6 and 6.7. Note that since we are only doing one proof, we use lower order approximations and smaller parameter domains. In fact we choose the lowest order for the four dimensional manifolds allowed by the non-resonance condition. This helps minimize the cost, in seconds, of computing the higher dimensional manifold.

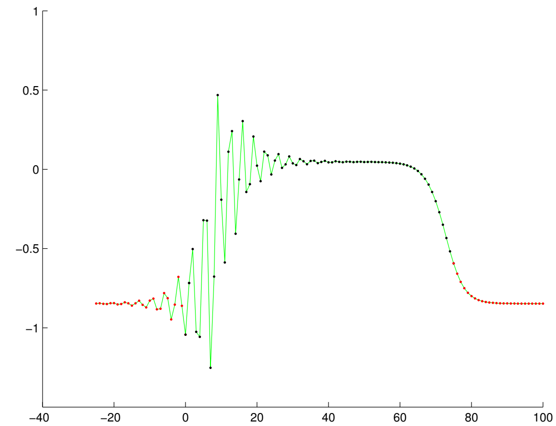

FIG. 6.3. *x-axis projection of the validated homoclinic;* $k = 75$, $\epsilon = 0.2$

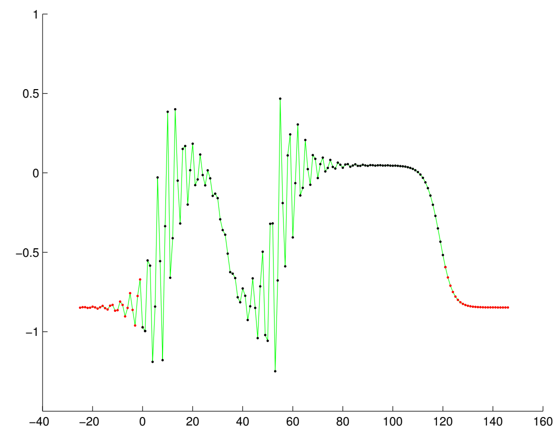

FIG. 6.4. *x-axis projection of the validated homoclinic;* $k = 121$, $\epsilon = 0.2$

7. Conclusions.

REFERENCES

[1] L. V. Ahlfors. Complex Analysis. An Introduction to the Theory of Analytic Functions of One Complex Variable. Third Edition. International Series in Pure and Applied Mathematics. *McGraw-Hill Book Co.*, New York, 1978.

[2] G. Arioli. Periodic Orbits, Symbolic Dynamics and Topological Entropy for the Restricted 3-Body Problem. *Comm. Math. Phys.* 231 (2002), no. 1, 1-24.

[3] G. Arioli, and P. Zgliczyński. Symbolic dynamics for the Hénon-Heiles Hamiltonian on the Critical Level. J. Differential Equations 171 (2001), no.1, 173-202.

[4] G. Arioli, and P. Zgliczyński. The Hénon-Helies Hamiltonian Near the Critical Energy Level-Some Rigorous Results. *Nonlinearity* 16 (2003), no. 5, 1833-1852.

[5] I. Baldomá, E. Fontich, and R.de la Llave. The Parameterization Method for One-Dimensional Invariant Manifolds of Higher Dimensional Parabolic Fixed Ponts *Discrete and Continuous Dynamical Systems* Vol 17 (4) , pp. 835–865, (2007).

Dim	Order	Approx Time	Proof Time	Validated Error	Radius	$\lvert\xi\rvert$	$\lVert\cdot\rVert_\nu$
2	9	5.1 sec	0.43 sec	4.95×10^{-13}	0.001	1.4	1.46×10^{-3}
4	5	11.3 sec	1.5 sec	2.96×10^{-12}	0.001	0.4	7.1×10^{-4}

TABLE 6.6

Manifold Validation Performance: Six Dimensional Example.

K	$\hat{x}_1$	r	time
20	$\begin{pmatrix} -2.743916182731272 \\ -2.745285611304841 \\ -2.745493386071762 \\ -2.868750115142552 \\ -2.869921042268439 \\ -2.870035612699910 \end{pmatrix}$	1.49×10^{-11}	4.4 sec

TABLE 6.7

Primary Intersection Validation: Six Dimensional Example.Chaos confirmed. The similarity in the coordinates of x_1 is due to the fact that the orbit begins close to the fixed point.

[6] J.B. van den Berg, J.P. Lessard, K. Mischaikow, and J.D. Mireles James. Rigorous numerics for symmetric connecting orbits: even homoclinics of the Gray-Scott. *To appear: SIAM J. on Math. Analysis* Preprint available at: www.math.rutgers.edu /~jmireles / grayScottPage.html

[7] W. Beyn, and J. Kleinkauf. The Numerical Computation of Homoclinic Orbits for Maps. *SIAM J. Numer. Anal.* 34 (1997), no.3, 1207-1236.

[8] W. Beyn, and J. Kleinkauf. Numerical Approximation of Homoclinic Chaos. Dynamical Numerical Analysis (Atlantl, GA, 1995). *Numer. Algorithms* 14 (1997), no. 1-3, 25-53.

[9] X. Cabré, E. Fontich, and R. de la Llave. The Parameterization Method for Invariant Manifolds. I. Manifolds Associated to Non-resonant Subspaces. *Indiana Univ. Math. J.*, 52(2):283-328, (2003).

[10] X. Cabré, E. Fontich, and R. de la Llave. The Parameterization Method for Invariant Manifolds. II. Regularity with Respect to Parameters. *Indiana Univ. Math. J.*, 52(2):329-360, (2003).

[11] X. Cabré, E. Fontich, and R. de la Llave. The Parameterization Method for Invariant Manifolds. III. Overview and applications. *J. Differential Equations*, 218(2):444-515, (2005).

[12] R. Calleja, and R. de la Llave. Fast Numerical Computation of Quasi-Periodic Equilibrium States in 1D Statistical Mechanics, Including Twist Maps. *Nonlinearity* 22 (2009), no. 6, 1311-1336.

[13] R. Calleja, and R. de la Llave. A Numerically Accessible Criterion for the Breakdown of Quasi-Periodic Solutions and its Rigorous Justification. *Nonlinearity* 23 (2010), no. 9, 2029-2058.

[14] M. Capinski. Covering Relations and the Existence of Topologically Normally Hyperbolic Invariant Sets. *Discrete Contin. Dyn. Syst.* 23 (2009), no. 3, 705-725.

[15] M. Capinski, and P. Roldan. Existence of a Center Manifold in a Practical Domain Around L_1 in the Restricted Three Body Problem. (In Preparation: *http://arxiv.org/abs/1103.1970v1*)

[16] A. Celletti, and L. Chierchia. KAM Stability and Celestial Mechanics. *Mem. Amer. Math. Soc.* 187 (2007), no. 878, viii+134 pp.

[17] B. Coomes, H. Koçak, and K. Palmer. Homoclinic Shadowing. *J. Dynam. Differential Equations* 17 (2005), no.1, 175-215.

[18] S. Day, J.P. Lessard, and K. Mischaikow. Validated Continuation for Equilibria of PDEs. *SIAM J. Numer. Anal.* 45 (2007), no. 4, 1398-1424.

[19] S. Day, R. Frongillo, and R. Treviño. Algorithms for Rigorous Entropy Bounds and Symbolic Dynamics. *SIAM J. Appl. Dyn. Syst.* 7 (2008), no. 4, 1477-1506.

[20] H. Dullin, and J. Meiss. Quadratic Volume-Preserving Maps: Invariant Circles and Bifurcations. *SIAM J. Appl. Dyn. Syst.* 8 (2009), no. 1, 76-128.

[21] E. Fontich, R. de la Llave, and Y. Sire. A Method for the Study of Whiskered Quasi-Periodic and Almost-Periodic Solutoins in Finite and Infinite Dimensional Hamiltonian Systems. *Electronic Research Announcements in Mathematical Sciences* Vol 16, pp. 9-22, (2009).

[22] F. Gabern, Á. Jorba, and U. Locatelli. On the Construction of the Kolmogorov Normal Form for the Trojan Asteroids. *Nonlinearity* 18 (2005), no. 4, 1705-1734.

[23] M. Gidea, and P. Zgliczyński. Covering Relations for Multidimensional Dynamical Systems. *J. Differential Equations* 202 (2004), no.1, 59-80.

[24] M. Gidea and P. Zgliczyński. Covering Relations for Multidimensional Dynamical Systems. II. *J. Differential Equations*, 202(1):59–80, 2004.

[25] C. Grebogi, S. Hammel, J.A. Yorke, and T. Sauer. Shadowing of Physical Trajectories in Chaotic Dynamics: Containment and Refinement. *Phys. Rev. Lett.* 65 (1990), no. 13, 1527-1530.

[26] A. Guillamon and G. Huguet. A Computational and Geometric Approach to Phase Resetting Curves and Surfaces. *SIAM Journal on Applied Dynamical Systems*, Vol 8, Issue 3, pp. 1005-1042 (2009).

[27] Á. Haro, and R. de la Llave. A Parameterization Method for the Computation of Invariant Tori and Their Whiskers in Quasi-Periodic Maps: Numerical Algorithms. *Discrete Contin. Dyn. Syst. Ser. B* 6 (2006), no. 6, 1261-1300.

[28] Á. Haro, and R. de la Llave. A Parameterization Method for the Computation of Invariant Tori and their Whiskers in Quasi-Periodic Maps: Rigorous Results. *J. Differential Equations* 288 (2006), no. 2, 530-579.

[29] W. M Hirsch, and C.C. Pugh. Stable manifolds and hyperbolic sets. Global Analysis (Berkeley 1960), Proc. Sympos. Pure Math Vol 14, pp 133–163, 1970.

[Johnson and Tucker(2011)] Johnson T, Tucker W (2011) A note on the convergence of parametrised non-resonant invariant manifolds. Qual Theory Dyn Syst 10(1):107–121,

[30] L. V. Kantorovič. Functional Analysis and Applied Mathematics. (Russian) *Vestnik Leningrad. Univ.* 3, (1948). no. 6, 3-18.

[31] L.V. Kantorovič. Functional Analysis in Normed Spaces, Moscow, 1959. Translated from the Russian by D.E. Brown. Edited by A.P. Robertson. *International Series of Monographs in Pure and Applied Mathematics*, Vol. 46. *The Macmillan Co.*, New York, 1964.

[32] J. Kennedy, S. Koçak, and J.A. Yorke. A Chaos Lemma. *Amer. Math. Monthly* 108 (2001), no. 5, 411-423.

[33] J. Kennedy, and J.A. Yorke. Topological Horseshoes. *Trans. Amer. Math. Soc.* 353 (2001), no. 6, 2513-2530.

[34] R. de la Llave, A. González, A. Jorba, and J. Villanueva. KAM theory without action-angle variables, *Nonlinearity*, 18(2) pp. 855-895, (2005).

[35] R. de la Llave. A tutorial on KAM theory, Smooth ergodic theory and its applications (Seattle, WA, 1999), *Proc. Sympos. Pure Math.*, Vol 69, pp. 175-292, 2001.

[36] R. de la Llave, and J.D. Mireles James. Parameterization of Invariant Manifolds by Reducibility for Volume Preserving and Symplectic Maps, (to appear in Discrete and Continuous Dynamical Systems-A)

[37] J. P. England, B. Krauskopf, and H. M. Osinga. Computing one-dimensional stable manifolds of planar maps without the inverse, *SIAM Journal on Applied Dynamical Systems* 3(2): 161190, 2004.

[38] J. P. England, B. Krauskopf, and H. M. Osinga. Bifurcations of stable sets in noninvertible planar maps, *Int. J. Bifurcation and Chaos* 15(3): 891904, 2005.

[39] H. Lomelí, and J. Meiss. Quadratic Volume-Preserving Maps. *Nonlinearity* 11 (1998), no. 3, 557-574.

[40] J.D. Mireles James, and Hector Lomelí. Computation of Heteroclinic Arcs with Application to the Volume Preserving Hénon Family. *SIAM J. Applied Dynamical Systems*, Volume 9, Issue 3, pp 919-953, 2010.

[41] K. Mischaikow, and M. Mrozek. Chaos in the Lorenz Equations: A Computer Assisted Proof. II. Details. *Math. Comp.* 67 (1998), no. 223, 1023-1046.

[42] K. Mischaikow, M. Mrozek, A. Szymczak. Chaos in the Lorenz Equations: A Computer Assisted Proof. III. Classical Parameter Values. Special Issue in Celebration of Jack K. Hale's 70th Birthday, Part 3. (Atlanta, GA/Lisbon, 1998). *J. Differential Equations* 169 (2001), no. 1, 17-56.

[43] A. Neumaier, and T. Rage. Rigorous Chaos Verification in Discrete Dynamical Systems, *Physica D* 67 (1994), no. 4, pp 327-346.

[44] S. Newhouse, M. Berz, J. Grote, and K. Makino. On the Estimation of Topological Entropy on Surfaces. Geometric and probabilistic structures in dynamics, 243-270, *Contemp. Math.*, 469, *Amer. Math. Soc., Providence, RI,* 2008.

[45] J.M. Ortega. The Newton-Kantorovich Theorem. *Amer. Math. Monthly* 75 1968 658-660.

[46] K. J. Palmer. Exponential Dichotomies, the Shadowing Lemma and Transversal Homoclinic Points. Dynamics reporten, Vol. 1, 265-306, *Dynam. Report. Ser. Dynam. Systems Appl.*, 1, Wiley, Chichester, 1988.

[47] S. Rump. Verification Methods: Rigorous Results Using Floating-Point Arithmetic. *Acta Numer.* 19 (2010), 287-449.

[48] E. Sander. Hyperbolic sets for noninvertible maps and relations. *Discrete and Continuous Dynamical Systems*, 5(2):339-358, 1999.

[49] E. Sander Homoclinic tangles for noninvertible maps. *Nonlinear Analysis*, 41(1-2):259-276, 2000.

[50] T. Sauer, and J.A. Yorke. Rigorous Verrification of Trajectories for the Computer Simulation of Dynamical Systems. *Nonlinearity* 4 (1991), no. 3, 961-979.

[51] S. Smale. Diffeomorphisms with Many Periodic Points. 1965 Differential and Combinatorial Topology (A Symposium in Honor of Marston Morse) pp. 63-80 *Princeton Univ. Press*, Princeton, N.J.

[52] J.C. Sprott. High-Dimensional Dynamics in the Delayed Hénon Map. *Electronic Journal of Theoretical Physics* 3 (2006), no. 12, 19-35.

[53] D. Stoffer, and K. Palmer. Rigorous Verification of Chaotic Behavior of Maps Using Validated Shadowing. *Nonlinearity* 12 (1999), no. 6, 1683-1698.

[54] A. Szymczak. The Conley Index for Decompositions of Isolated Invariant Sets. *Fund. Math.* 148 (1995), no. 1, 71-90.

[55] W. Tucker. A Rigorous ODE Solver and Smale's 14th Problem. *Found. Coumpt. Math.* 2 (2002), no. 1, 53-117.

[56] D. Wilczak. Abundancs of Heteroclinic and Homoclinic Orbits for the Hyperchaotic Rössler System. *Discrete Contin. Dyn. Syst. Ser. B 11* (2009), no. 4, 1039-1055.

[57] A. Wittig, M. Berz, J. Grote, K. Makino, and S. Newhouse. Rigorous and Accurate Enclosure of Invariant Manifolds on Surfaces. *Regul. Chaotic Dyn.* 15 (2010), no. 2-3, 107-126.

[58] G. Zbigniew, and P. Zgliczyński. Abundance of Homoclinic and Heteroclinic Orbits and Rigorous Bounds for the Topological Entropy for the Hénon Map. *Nonlinearity* 14 (2001), no. 5, 909-932.

[59] P. Zgliczyński. Covering Relations, Cone Conditions and the Stable Manifold Theorem. *J. Differential Equations*, 246(5):1774–1819, 2009.